A NEW BIFUNCTIONAL CHELATING LIGAND BASED ON GLUCOSAMINE FOR THE $[M(CO)_3]^+$ (M =Tc, Re) CORE

by

CHARLES BETHUNE EWART

B.Sc., The University of British Columbia, 2002

A THESIS SUBMITTED IN PARTIAL FULFILLMENT OF THE REQUIREMENTS FOR THE DEGREE OF

MASTER OF SCIENCE

in

THE FACULTY OF GRADUATE STUDIES

(Chemistry)

THE UNIVERSITY OF BRITISH COLUMBIA

June 2006

ABSTRACT

The development of a SPECT (single photon emission computed tomography) carbohydrate analogue for FDG (2-deoxy-2-[^{18}F]fluoro-*D*-glucose), used in PET (positron emission tomography), is of great interest in the scientific community. The great utility of FDG suggests that other radiolabelled carbohydrates may be medicinally useful compounds. PET is expensive and not readily available, due to the inherent short half-lives and cyclotron production of the positron emitters. SPECT allows for the use of common radionuclides such as ^{99m}Tc, which is the most widely used radioisotope in nuclear medicine because of its near ideal imaging properties. This work describes the synthesis and characterization of a carbohydrate-appended tridentate ligand (H**L2**) designed for the $[M(CO)_3]^+$ (M = Tc, Re) core. This core is synthetically useful because it is small, robust, and will afford a neutral complex with the monoprotic H**L2** ligand. The complexation to produce the corresponding complexes M(**L2**)$(CO)_3$ (M = Tc, Re) was also undertaken, and Re(**L2**)$(CO)_3$ was characterized via ^{1}H and ^{13}C NMR spectroscopy, IR spectroscopy, mass spectrometry, and elemental analysis. Kit preparation of the precursor $[^{99m}Tc(CO)_3(H_2O)_3]^+$ species for radiotracer studies is well documented, and the cation can be prepared in high yield with excellent radiochemical purity. Labelling studies to produce ^{99m}Tc(**L2**)$(CO)_3$ indicated high radiolabelling yields, as determined by HPLC methods. Challenge experiments with aqueous solutions of cysteine and histidine indicate strong tridentate binding of H**L2** to the metal centres.

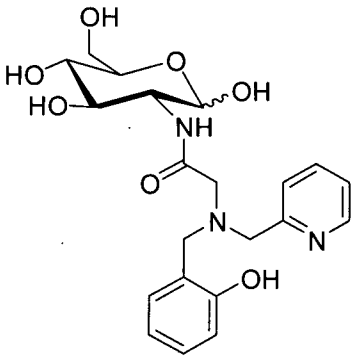

HL2

TABLE OF CONTENTS

LIST OF FIGURES

LIST OF SCHEMES

List of Abbreviations

Abbreviation/Symbol	Meaning
α	alpha particle, as in α-emission or α-decay
β	beta, as in β-emission or β-decay
β^+	positron
β^-	beta particle
δ	chemical shift in NMR spectroscopy, units are ppm
γ	gamma energy
λ	wavelength
AcOH	acetic acid
Ac_2O	acetic anhydride
APCI	atmospheric pressure chemical ionization
APT	attached proton test
BnBr	benzyl bromide
BBB	blood-brain-barrier
BFCA	bifunctional chelating agent
BOC	*tert*-butoxycarbonyl
br	broad
CBZ	N-benzyloxycarbonyl
COSY	correlation spectroscopy
cm^{-1}	wavenumber, in IR spectroscopy
d	doublet, in NMR spectroscopy
dd	doublet of doublets, in NMR spectroscopy

DCC	dicyclohexylcarbodiimide
DMAP	dimethylaminopyridine
DTPA	diethylenetriaminepentaacetate
EA	elemental analysis
E_β	beta energy
E_γ	gamma energy
EDC.HCl	*N*-(3-dimethylaminopropyl)-*N'*-ethylcarbodiimide hydrochloride
EDTMP	ethylenediaminetetramethylenephosphonate
ESIMS	electrospray ionization mass spectrometry
FDG	2-deoxy-2-[^{18}F]fluoro-*D*-glucose
FMOC	9-fluorenylmethoxycarbonyl
FT-IR	Fourier-transform infrared
Gln	glucosamine
GLY	glycine
GLUT1	glucose transporter 1
GLUT2	glucose transporter 2
GLUT4	glucose transporter 4
GLUTs	glucose transporters
HMQC	heteronuclear multiple quantum correlation
HR-MS	high resolution mass spectrometry
HOBt	1-hydroxybenzotriazole
HOBt.H_2O	1-hydroxybenzotriazole hydrate

HPLC	high pressure liquid chromatography
Hz	hertz
IR	infrared
J	coupling constant, in NMR spectroscopy
keV	kiloelectron volts
LR-MS	low-resolution mass spectrometry
M	i) central atom or parent peak in MS
	ii) concentration, in molarity
MH^+	*m/z* = weight of parent peak + proton, in MS
MNa^+	*m/z* = weight of parent peak + sodium, in MS
m	i) medium, in IR spectroscopy
	ii) multiplet, in NMR spectroscopy
mCi	millicurrie, a measure of radioactivity
mmol	millimole
mol	mol
m/z	mass to charge ratio, in MS
MRI	magnetic resonance imaging
MS	mass spectrometry
NMR	nuclear magnetic resonance
2-pca	2-pyridinecarboxaldehyde
PBS	phosphate buffer saline
PET	positron emission tomography
ppm	parts per million, in NMR spectroscopy

R_f	retention factor in TLC
s	i) strong, in IR spectroscopy
	ii) singlet, in NMR spectroscopy
sal	salicylaldehyde
SPECT	single photon emission computed tomography
t	triplet, in NMR spectroscopy
td	triplet of doublets, in NMR spectroscopy
$t_{1/2}$	half-life
t_R	retention time, in HPLC
TFA	trifluoroacetic acid
TLC	thin layer chromatography
U.S. FDA	United States Food and Drug Administration
w	weak, in IR spectroscopy
ν_{max}	position of IR peak, units are cm^{-1}

ACKNOWLEDGEMENTS

First and foremost, I would like to thank Dr. Chris Orvig for taking me into his group and allowing me to pursue this degree and Dr. Mike Adam (TRIUMF) for such an interesting project. Their knowledge and enthusiasm for the subject has made my experience both interesting and challenging. Three thanks: one to Dr. Tim Storr, for introducing me to D419 during my start and for all the help a lab mate could ask for; one to Dr. Neil Lim for his patience and guidance during his stay here in our group; and one to Cara Ferreira (HPLC, radiolabelling, TRIUMF) for all her help with the radiolabelling process. I would like to thank the current members of Équipe Orvig (Kathie, Cheri, Meryn, and Lauren) for an enjoyable working environment and to all the people in the office, shops, and services here in the UBC Chemistry department (NMR, mass spec, EA, glass shop) for their help. Last, and not least, a special thanks goes out to my friends and family, especially Alison Lee and Bubs (Carli), for their love and support.

CHAPTER 1: INTRODUCTION

1.1 Bioinorganic and medicinal inorganic chemistry

Bioinorganic chemistry concerns the involvement of metal ions in biological systems; it is the hybrid of biology and inorganic chemistry. Medicinal inorganic chemistry is the branch of bioinorganic chemistry involving the application of inorganic chemistry to the diagnosis and therapy of disease.[1] The periodic table contains many metals with varied properties. As such, different metals can be invoked in medicinal inorganic chemistry depending on the properties and characteristics that are required of a potential diagnostic or therapeutic agent. Furthermore, such metals can be radioactive or non-radioactive, and the corresponding complexes can be tuned depending on the particular nature of the metal ion. For example, MRI (magnetic resonance imaging) utilizes the trication of Gd, which is chosen for this particular technique because of its unique magnetic properties (*i.e.* Gd^{3+} has 7 unpaired electrons).[2] In particular, nuclear medicine employs radioactive metals for diagnosis and therapy. For example, ^{99m}Tc ($t_{1/2}$ = 6 h, E_γ = 141 keV) can be used for SPECT (single photon emission computed tomography), and ^{68}Ga (β^+, $t_{1/2}$ = 1.1 h, E_γ = 511 keV) can be used for PET (positron emission tomography). Thus, chemists are given the opportunity to design drugs to target particular organs or tissues.

1.2 Carbohydrates and transport

Carbohydrates are the principal energy source of the body's organs, tissues, and cells, such as the brain.[3] The breakdown of carbohydrates into glucose **1** and other monosaccharides (e.g. galactose **2**, mannose **3**, and glucosamine **4**, and fructose **5**)

(Figure 1-1, showing D-sugars) occurs extracellularly.[3] Because cell membranes and the blood-brain-barrier (BBB) are essentially impermeable to monosaccharides, specialized transporters (collectively called glucose transporters or GLUTs) are present to enable their passage into the cell.[4, 5] In particular, studies have indicated that extracellular glucosamine transport is maintained by GLUT2,[6] but is also regulated by GLUT1 and GLUT4, for transport intracellularly across the BBB.[7]

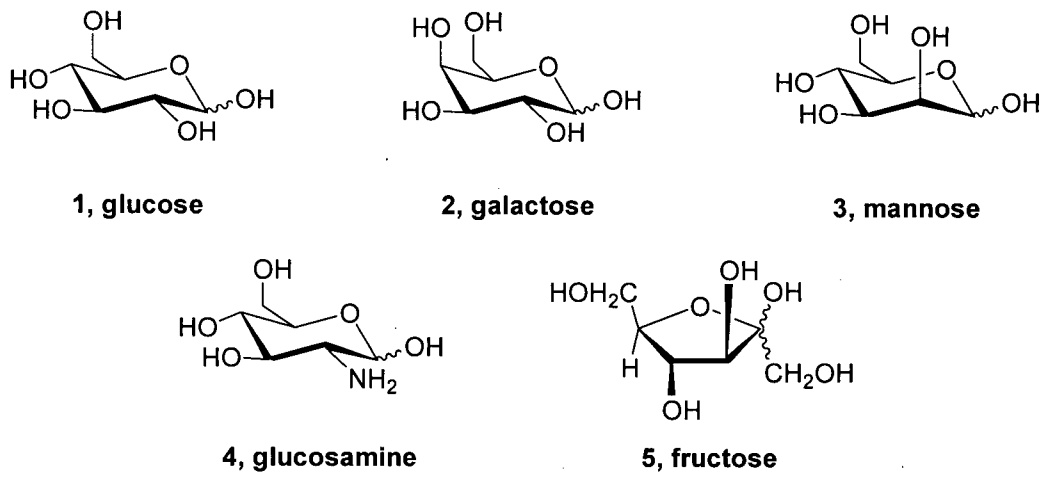

Figure 1-1. Some naturally occurring D-monosaccharides

1.3 Inorganic Drugs

Inorganic drugs are drugs that contain inorganic elements such as a metal ion. Inorganic drugs are comprised of two types: diagnostic drugs and therapeutic drugs.[1, 8] There have been several review articles that describe metallodrugs,[9] and some examples are shown in Figure 1-2. Diagnostic drugs can include radiopharmaceuticals, such as Cardiolite® (^{99m}Tc-Sestamibi) **6** for SPECT heart imaging in cardiac patients, MRI contrast agents, such as $[Gd(DTPA)(H_2O)]^{2-}$ (DTPA = diethylenetriaminepentaacetate) (Magnevist®)[2] **7**, and metal-based X-ray contrast agents, for instance $BaSO_4$.[10] Examples of therapeutic drugs include radiopharmaceuticals, such as Quadramet®

(^{153}Sm-EDTMP)[10] (EDTMP = ethylenediaminetetramethylenephosphonate) for palliative treatment of bone pain and Zevalin® (^{90}Y-ibritumomab tiuxetan) for non-Hodgkin's lymphoma, and metal-containing drugs,[10] such as Auranofin **8** for arthritis and Cisplatin **9** for cancer treatments.

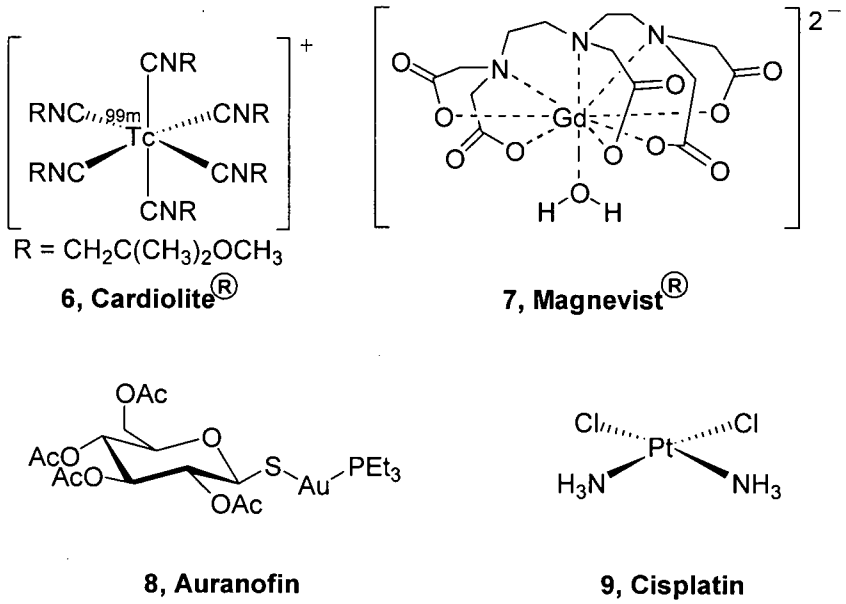

Figure 1-2. Some inorganic drugs used in medicine

Essentially, diagnostic drugs are designed to determine what is wrong with (or within) a patient. Therapeutic drugs, on the other hand, are designed to travel to a target organ or tissue and either treat the diseased area or bind to the harmful material and aid in its removal from the body. Such compounds include radiopharmaceuticals that can deliver *in vivo* radiation therapy (relevant radionuclide processes include α or β decay),[11] chemotherapeutics, and chelating agents.[9] The group 7 transition metals, Tc for diagnosis and Re for therapy, have been the focus of much research in recent years and form a template onto which potentially useful radiopharmaceuticals in our group are being built.[12-15]

1.4 Nuclear medicine and radiopharmaceuticals

In medicine, a modality is a therapeutic method or agent, such as surgery or chemotherapy, which involves the physical treatment of a disorder. Nuclear medicine is a functional imaging modality, and as such, involves targeting molecules with radiopharmaceuticals for the diagnosis and treatment (therapy) of disease.[1, 8, 11] Radiopharmaceuticals are radionuclide containing drugs, which are routinely used in the nuclear medicine department of a hospital.[1, 8] These provide relatively non-invasive procedures (one sees the result of their actions via an external detector) and insights into either the biochemical or metabolic processes present within an individual. Two diagnostic radiopharmaceuticals are FDG (2-deoxy-2-[^{18}F]-*D*-glucose) **10** for PET brain imaging in Alzheimer and Parkinson patients, and Cardiolite® **6**, for SPECT evaluation of coronary blood flow. FDG is the only U.S. FDA (United States Food and Drug Administration) approved PET imaging agent, whereas Cardiolite® is an example of a commercially available SPECT imaging agent.

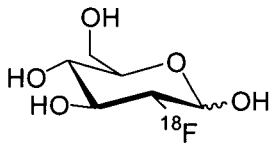

10, FDG

Furthermore, radiopharmaceuticals are radioactive compounds which, when administered for purposes of diagnosis and therapy, typically do not elicit any physiological or pharmacological response from the patient.[8] These compounds are administered in low concentrations, almost exclusively by intravenous injection, but can also be introduced by inhalation or ingestion, depending on the chemical nature of the radiopharmaceutical. Information about the physiological process of interest is obtained through imaging by emission tomography. All radionuclides commonly administered to patients in a nuclear medicine department are artificially produced by, or isolated from,

cyclotrons, nuclear reactors, or radionuclide generators. Using external imaging devices, one can follow the decay of radioactive tracers *in vivo* and their fate due to the physiological response of the body as the biodistribution of a radionuclide is dependent on its uptake and delivery to the intended target.[11] Most often, a ligand is designed to bring the radioactive isotope directly to the diagnostic or therapeutic site. Ideally, radiopharmaceuticals should have a low radiation dose, a high activity, a minimum hazard risk to patient and technician, a convenient synthesis and administration, and be cost-effective.

1.5 Radioactive decay in nuclear medicine

In general, radioactive decay is the spontaneous decay of certain nuclei, accompanied by emission of a particle and/or a photon. It is the emission of a particle that can be potentially harnessed in therapeutic radiopharmaceuticals and the emission of a photon that can be utilized in diagnostic radiopharmaceuticals. Therapeutic radiopharmaceuticals are designed to destroy harmful tissue. Generally, these compounds contain radionuclides that decay by either α- or β-emission. Alpha decay is the emission of an α-particle (or He nucleus) consisting of two protons and two neutrons. Beta decay is the emission of a high energy electron from the nucleus. Diagnostic radiopharmaceuticals contain radionuclides that decay by either gamma (γ) or positron (β^+) emission. In the former case, the parent is in an excited state that does not isotopically change when converted to the daughter nucleus. The decay process is accompanied by the emission of a photon. In the latter case, a proton from the parent nucleus is converted into a neutron by emission of a positron, forming the daughter nucleus. Compounds incorporating gamma- or positron-emitting radionuclides are

designed to determine the nature of a disease (*i.e.* a symptom or distinguishing feature) that serves as supporting evidence during an examination of a patient. While providing a non-invasive means of assessing the physiology and morphology of organs and tissues, these compounds are thus important in the diagnosis of disease and provide an additional means of monitoring and assessing the use and progress of treatment strategies. There are two general techniques available for producing diagnostic images in nuclear medicine: PET, which utilizes positron-emitting radionuclides, and SPECT, which utilizes gamma-emitting radionuclides. In both techniques, the distribution of the radiotracer over time during subsequent uptake by the target organ is imaged by emission tomography and used to obtain information about the physiological process of interest.

1.6 Diagnosis in nuclear medicine via PET and SPECT

As discussed above, PET and SPECT are *in vivo* diagnostic imaging methods that differ in their choice of radioisotope. Each technique detects radiation and produces a diagnostic image. Without highly invasive surgical procedures, these imaging methods are able to address anatomical structure, metabolic function, and offer tomographic data by following the time course of the radioactive tracer *in vivo*. The sensitivity and sophistication of the imaging machines allows for the planar (two-dimensional) or tomographic (three-dimensional) distribution of radioactivity to be inferred from outside the body. This is in contrast to an X-ray scan, which transmits an external source of radiation through the patient to create a planar view of the inside of the body. As will be discussed, even though similar principles exist to create and produce the images, the differences between PET and SPECT originate in their choice of radioisotope, and the utility of each technique is inherently limited by this fact.

SPECT is a tomographic method used for imaging local metabolic and physiological functions in tissues. It differs from PET because it is only able to detect a single gamma photon from each nuclear disintegration and thus, generates a lower-quality image. SPECT utilizes routinely available γ-emitting radionuclides, resulting in its widespread use in nuclear medicine. Examples include ^{67}Ga ($t_{1/2}$ = 78.3 h, E_γ = 296, 185, 93 keV), ^{99m}Tc ($t_{1/2}$ = 6.0 h, E_γ = 141 keV), and ^{111}In ($t_{1/2}$ = 67.9 h, E_γ = 245, 172 keV).[16] The subsequent decay of an excited state to a ground state is accompanied by the emission of a photon (γ), which is detected by the SPECT camera. SPECT is sufficiently sensitive for routine uses in nearly all the same applications as PET, despite the inherent lowered sensitivity resulting from the emission of a single photon. In addition, the cost of a SPECT scan is considerably less than that of a PET scan, the infrastructure for SPECT scans already exists in most major hospital nuclear medicine facilities, and certain SPECT radioisotopes (*e.g.* ^{99m}Tc) can be generator-produced.

PET is similar to SPECT because it can obtain a picture of the metabolic function of the body. The biochemical activity within the body is imaged through the detection of gamma rays that are emitted when introduced radionuclides decay and release positrons. The interaction of the positron with an electron creates an annihilation event, whereby the conversion of matter to energy results in two 511 keV γ-rays oriented 180° apart. Incorporation of such radioisotopes into radiopharmaceuticals and their functional utility is limited by their short half-lives. Examples of some biologically relevant PET radioisotopes are ^{11}C ($t_{1/2}$ = 20 min), ^{13}N ($t_{1/2}$ = 10 min), ^{15}O ($t_{1/2}$ = 2 min), and ^{18}F ($t_{1/2}$ = 110 min). One advantage of such short-lived radioisotopes is the low radiation dose for the patient from a relatively large dose of radiopharmaceutical, which results in higher

quality images. Despite excellent resolution and sensitivity, this technique lacks practicality and does not allow technicians to handle large volumes of patient cases due to the fact that a nearby cyclotron is required to produce the short-lived radioisotopes. Furthermore, unlike SPECT, which images the site of γ-emission, PET images the site of β^+-annihilation. Compounding this lack of availability for patients is the cost of a PET scan (in the thousands of dollars) and the fact that this cost is not usually covered by the Canadian medical system.

1.7 FDG as a template for a SPECT radiopharmaceutical

FDG **10** is widely used as a PET imaging agent.[17, 18] It is able to cross the BBB through active transport where it is phosphorylated by hexokinase;[3] however, metabolism stops because the phosphorylated FDG is unable to undergo further modification and the compound builds up in the cell.[18] Compensating for the half-life of ^{18}F, procedures now exist to synthesize FDG in as little as 30 minutes, optimizing the activity available.[17] It is this success of FDG as a PET imaging agent that has suggested that radiolabelled carbohydrates may be useful in developing an FDG-analog for SPECT applications. In addition, commercial considerations also include radionuclide availability and ease of preparation of the radionuclide (*i.e.* generator produced); it is the SPECT radioisotope ^{99m}Tc ($t_{1/2}$ = 6.0 h, E_γ = 141 keV) that can satisfy the radionuclide requirements (*i.e.* reasonable half-life, sufficient energy, ease of preparation). FDG can serve as a template when designing a potential radiopharmaceutical candidate based on glucosamine **4**, *i.e.* the induced functionality

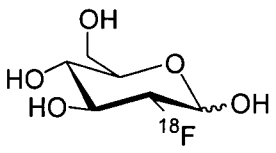

10, FDG

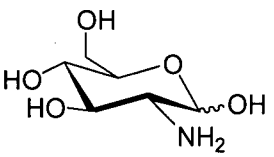

4, glucosamine

occurs at the C2 site. Furthermore, the amine moiety in glucosamine can be functionalized with an amine or an amide bond. The development of a SPECT analogue for PET-FDG (*i.e.* a compound with similar activity and specificity) would be extremely practical and useful, and would be a major breakthrough in developing a new area of SPECT radiopharmaceuticals.[19] In addition, Re, a congener of Tc, may be used as a dual diagnostic/therapeutic agent since the two Re isotopes (^{186}Re and ^{188}Re) each have both gamma and beta decays.

1.8 Technetium and rhenium

Technetium is the most widely used element in nuclear medicine, almost exclusively as the radioisotope ^{99m}Tc;[20] over 85% of all diagnostic nuclear medicine scans use ^{99m}Tc in some chemical form.[21] All radioisotopes of technetium are radioactive and they all have a low radiation burden and high efficiency detection. Hence, it is possible to inject at least 20 mCi with low radiation exposure to the patient.[22] ^{99m}Tc ($t_{1/2}$ = 6.0 h, E_γ = 141 keV) is an excellent candidate for diagnostic and imaging purposes because it has a near ideal half-life, a sufficient γ-ray energy, and is generator-produced (^{99}Mo/^{99m}Tc generator).[8] Such a radioisotope is sufficiently long-lived to allow chemical modification to occur before too much decay has occurred. Thus, ^{99m}Tc is relatively inexpensive, convenient, and widely available.[21] ^{99m}Tc is produced from a ^{99}Mo/^{99m}Tc generator, which is the most prominent generator in nuclear medicine. However, the short-half life of ^{99m}Tc makes it impractical to store it even on a weekly basis. This problem of supply is overcome by obtaining the parent ^{99}Mo ($t_{1/2}$ = 67 h) and eluting and collecting the continuous production of ^{99m}Tc from a radionuclide generator. This allows nuclear medicine departments the practicality of obtaining short-lived radionuclides

without having to be in close proximity to a cyclotron. The parent molybdenum-99 radionuclide, obtained as the molybdate anion $[^{99}MoO_4]^-$, can be packaged and transported in generator-form to a nuclear medicine department. The ^{99m}Tc is obtained as the pertechnetate anion, $[^{99m}TcO_4]^-$, off the generator column (alumina) in aqueous solution after elution with 0.9% saline. Any chemistry performed must manipulate $[^{99m}TcO_4]^-$ in this aqueous form and reduce ^{99m}Tc(VII) to a more manageable oxidation state. For example, by reducing $[^{99m}TcO_4]^-$ using $NaBH_4$ under a CO atmosphere, the Tc(I) complex cation $[^{99m}Tc(CO)_3(H_2O)_3]^+$ is formed.[23]

Rhenium is the third row analogue of technetium and occurs naturally as a mixture of two non-radioactive isotopes, ^{185}Re (37.4%) and ^{187}Re (62.6%). Rhenium has the potential to be both a diagnostic and a therapeutic agent. Its two radioisotopes, ^{186}Re ($t_{1/2}$ = 90 h, E_β = 1.07 MeV, E_γ = 137 keV) and ^{188}Re ($t_{1/2}$ = 17 h, E_β = 2.1 MeV, E_γ = 155 keV), both have a primary β-emission and a secondary γ-decay which could be harnessed for therapy and diagnosis, respectively.[9,20] Each radioisotope has an appropriate half-life, a high energy of β-particle emission, and an ideal energy of γ-photon emission decay. ^{188}Re can be produced by neutron capture on ^{187}Re or through the use of a $^{188}W/^{188}Re$ generator. ^{186}Re can only be produced by irradiating ^{185}Re with neutrons. Despite the radioisotopic characteristics, it is the generator production of ^{188}Re that makes it more appealing than neutron capture reactions. In addition, since Tc and Re are in the same period, it is expected that Tc and Re will have similar chemical properties and react similarly with the same ligands.[24] The major disadvantage to the production of ^{186}Re and ^{188}Re by neutron radiation is the inevitable contamination with the non-radioactive ^{185}Re and ^{187}Re isotopes, respectively.[24]

1.9 $[M(CO)_3(H_2O)_3]^+$ (M = Tc, Re) core

The development of the $[M(CO)_3(H_2O)_3]^+$ (M = Tc, Re) core has opened up a new area of potential radiopharmaceutical candidates, and several reviews exist on the use of such an organometallic core.[8, 25-28] The advantages of this compound are that it is stable, kinetically inert (for *fac*-$[Tc(CO)_3]^+$), and of small size. Pioneered by Alberto,[23, 29] $[^{99m}Tc(CO)_3(H_2O)_3]^+$ **11** is synthesized from $[^{99m}TcO_4]^-$ under atmospheric pressure in the presence of saline via a kit formulation (Isolink®, Malinckrodt, Inc.)[30, 31] shown in Scheme 1-1. This simple preparation involves a boranocarbonate complex which acts as a dual functioning CO-source and reducing agent.[29] This is nice synthetically because it only takes a few hours to make the complex and effectively label the ligand system.[29, 30]

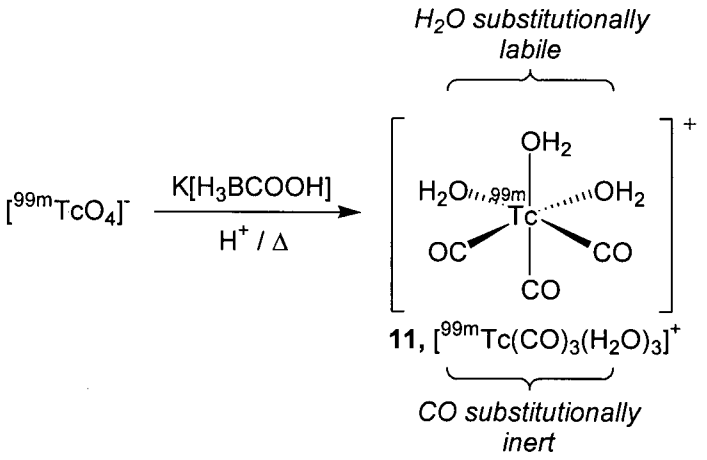

Scheme 1-1. Preparation of $[^{99m}Tc(CO)_3(H_2O)_3]^+$ **11** via the Isolink® kit

The core has Tc(I) in a low spin d^6 electron configuration, CO ligands which are inert to substitution, and H_2O ligands which are labile to substitution (CO, being a stronger π–acceptor, is able to labilize the H_2O ligand trans to it) by amines (*e.g.* heterocyclic, aromatic, and aliphatic amines), carboxylates, carbonyls, and alcohols (*e.g.* phenols). In developing ligand systems, one hopes to functionalize via a closed

coordination sphere.[30] Such functionalization (Figure 1-3) can occur via monodentate (imidazole, **12**), bidentate (2-picolylamine-N-acetic acid, **13**), or tridentate ligands (histidine, **14**).[7]

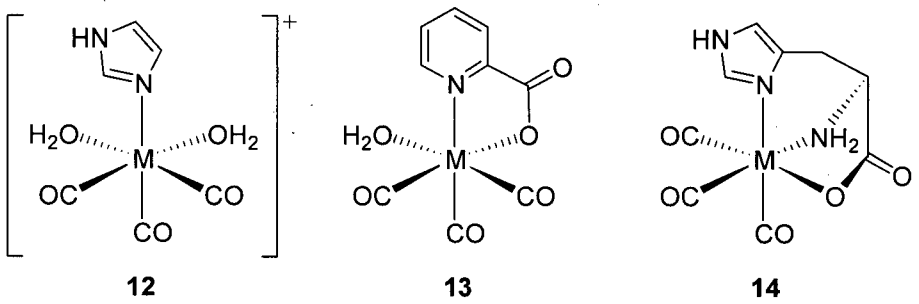

Figure 1-3. Functionalization of $[M(CO)_3]^+$ (M = Tc, Re) with various ligand types

As seen in Figure 1-3, a monodentate ligand replaces one H_2O ligand; this is useful when studying a [2+1] mixed ligand concept, where a monodentate ligand can be used to trap a bidentate co-ligand complex that can represent the variable portion of a radiolabeled biomolecule.[32] Bidentate ligands result in an open coordination site, which can be occupied by a solvent molecule (*i.e.* H_2O or MeOH), a halide (*i.e.* Cl^- or Br^-), or a monodentate ligand. As a result, such complexes show aggregation with plasma proteins *in vitro* and *in vivo*, and therefore are retained in the blood and kidneys.[33, 34] Bidentate complexes also are not very stable to challenge experiments with cysteine and histidine; the amino acid readily displaces the bidentate ligand from the core and inevitably results in complex decomposition.[14] Tridentate ligands, on the other hand, create a closed coordination environment around the tricarbonyl core. The resulting complexes (Figure 1-4) can be neutral (for example, with a monoanionic ligand picolylaminediacetic acid, **15**),[7] anionic (for example, with a dianionic ligand iminodiacetic acid, **16**),[7] or cationic (for example, with a neutral ligand N-(pyridine-2-ylmethyl)ethane-1,2-diamine, **17**).[35]

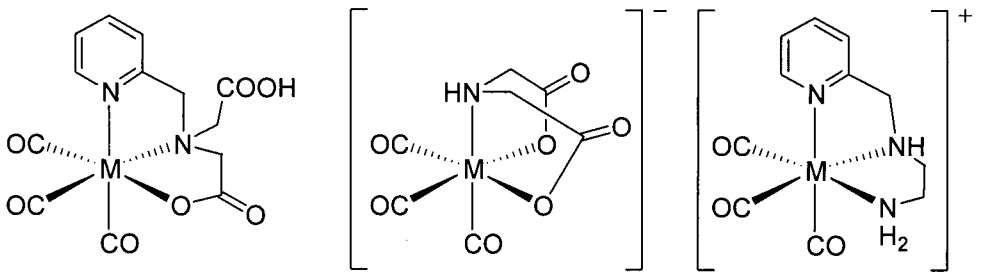

Figure 1-4. Examples of neutral, anionic, and cationic (M = Tc, Re) tricarbonyl complexes

The *fac*-$[^{99m}Tc(CO)_3]^+$ moiety is quite versatile, forming thermodynamically stable complexes with tridentate ligand systems, especially those incorporating histidine, cysteine, polyamines, and pyridine.[27, 36] Various tridentate systems have been investigated, among those aromatic, thioether/thiol, [37, 38] and thiosemicarbazones.[38, 39] Further tridentate systems include a maleimide group for binding to thiol groups,[40, 41] cationic amine ligands,[35] S-functionalized cysteine,[42] and a carborane complex.[43] Such tridentate complexes have their donor ligands occupying all three available coordination sites, resulting in closed shell 18-electron complexes that are stable to hydrolysis and are formed very efficiently and effectively.[36]

As can be seen in Figure 1-4, all three of the tridentate ligands have a secondary or tertiary N atom that acts as a neutral donor (in **15**, the tertiary N is functionalized with an acetic acid residue). Such a ligand is called a bifunctional chelating agent (BFCA) because the secondary or tertiary N can be further functionalized and attached to a biomolecule (*i.e.* amino acid or carbohydrate), while chelating the radioactive isotope. The facile preparation of a BFCA with a pendent amino or carboxylic acid functionality for coupling via an amide bond has been demonstrated recently.[44] The testing of

potential BFCAs with bidentate and tridentate ligand systems has resulted in better pharmacokinetic profiles for biologically relevant tridentate ligands.[7]

When amino acids are the biological molecule, such systems are referred to as single amino acid chelates (SAAC).[45, 46] The *fac*-$[^{99m}Tc(CO)_3]^+$ moiety has a strong affinity for histidine residues in proteins and peptides.[26, 47] As a result, compounds containing histidine or histidine-functionalized ligands have been synthesized, and challenge experiments against this ubiquitous amino acid are undertaken to determine thermodynamic stability. For example, histidine can be incorporated into BFCAs[31, 48] and synthetic peptides with high specific activities;[49] histidine-functionalized ligands include a vitamin B_{12}-conjugate containing an N_ε-functionalized histidine.[50] The labeling of small peptides by solid-phase synthetic methods has also been explored with the incorporation of pyridyl, imidazole, and/or carboxylate groups into derivatized or synthetic amino acid analogues.[46, 51, 52] One example involves combining fluorescence and radioimaging into one bifunctional tridentate ligand,[53] while a recent example includes incorporating amino acid chelators into monosaccharide-containing compounds.[54] Some ^{99m}Tc complexes have been made that are either ionic or have quite high molecular weights, which are a disadvantage in living systems.[55, 56] This can be avoided by introducing simple N,O donor ligands; such systems with the *fac*-$[M(CO)_3]^+$ (M = Tc, Re) core can possess intermediate lipophilicity,[18] which is an advantage in living systems.

The *fac*-$[Re(CO)_3(H_2O)_3]Br$ precursor can be prepared in almost quantitative yield by refluxing $[Re(CO)_5]Br$ in H_2O for 24 h.[57] ^{188}Re may soon be more available, as the preparation of the $[^{188}Re(CO)_3(H_2O)_3]^+$ in kit form from aqueous media has recently

been presented.[58] This precursor cation has been used in conjunction with bis-imidazole and bis-acid ligands forming complexes in high yield; these ligands could show versatility and length of spacer adaptability to various biomolecules[58] and the complexes may target small peptides and eventually expand to the ^{99m}Tc radioconjugates.[59]

1.10 Thesis focus and design

This project began in our group with the idea to develop glucose-containing bifunctional chelators for the $[M(CO)_3(H_2O)_3]^+$ core (M = Tc, Re).[8, 26] The concept was to develop a ligand with a pendant carbohydrate as a targeting molecule, an amino acid as a linker, and a tridentate scaffold as a chelator (Figure 1-5).

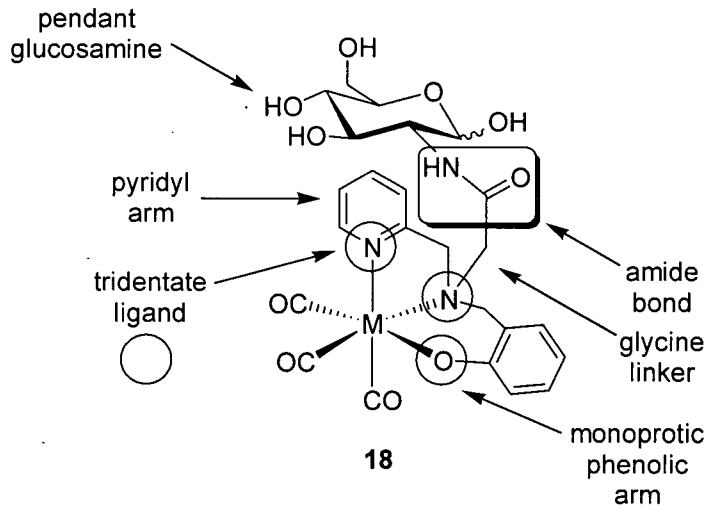

Figure 1-5. Ligand design incorporated in this thesis (M = Tc, Re)

For the pendant carbohydrate, glucosamine **4** was chosen. As in FDG **10**, glucosamine has its functionality at C2; in this case, the OH group is replaced by an NH_2. This is important synthetically because not only can glucosamine act as a vector to deliver a potential target radionuclide, but the C-2 amine group can be functionalized with an amine or an amide bond and act as a linkage site. Furthermore, in support for the

metabolism of glucosamine, evidence in the literature suggests that glucose transporters and hexokinase are active towards N-functionalized glucosamines.[4, 6, 7] This is essential if such a compound is to be a successful biomedical candidate. The carbohydrate is kept pendant by a glycine spacer (that could be extended with various methylene chains) that is modifiable in length. The tertiary nitrogen of the glycine spacer can be further functionalized with various aromatic arms (*e.g.* pyridine, histidine) and monoprotic arms (*e.g.* phenol, acetic acid) to create a tridentate binding site for the tricarbonyl core, thus creating a bifunctional chelate. The aromatic arm could be installed using a reductive amination[60] and involves a heterocyclic amine donor, which has shown high affinity for Tc-99m in its +1 oxidation state. The final tridentate binding site would be monoprotic carboxylate group (via an N-alkylation)[61, 62] or a phenolate group (via reductive amination)[60] to create an overall neutral complex when bound to the metal centre. Other tridentate pendant carbohydrate ligands have been synthesized and investigated, including functionalization of glucose at C3 (with imidazole, pyridine, and carboxylic acid via an ether linkage)[63] and *in vitro* studies against GLUT1 and hexokinase of functionalized glucose via ether linkages at C1, C2, C3, and C6 with various chelating systems.[64]

The ligand progression (Figure 1-6) and investigation of carbohydrate-appended metal complexes in our lab began with the synthesis of a bidentate Schiff base compound via a condensation of glucosamine with salicylaldehyde **19**.[12] Such a ligand has been investigated for ^{99m}Tc(V).[65, 66] Unfortunately, the imine **19** and its resulting complex were unstable to hydrolysis, making such a ligand unsuitable for aqueous chemistry.[12] The hydrolysis problem was circumvented by reducing the imine to the more

hydrolytically robust amine phenol **20**. The goal was to make a bidentate complex; however, ^{13}C NMR spectroscopy showed that the amino N, phenolato O, ***and*** the C3 hydroxyl O groups bound the metal in a tridentate fashion. Despite the tridentate binding, the complex was unstable to challenge experiments (cysteine and histidine), implying that a more directed approach to an actual tridentate ligand was needed; *i.e.* the carbohydrate moiety needed to remain pendant and the ligand structure required modification to ensure a tridentate binding motif.

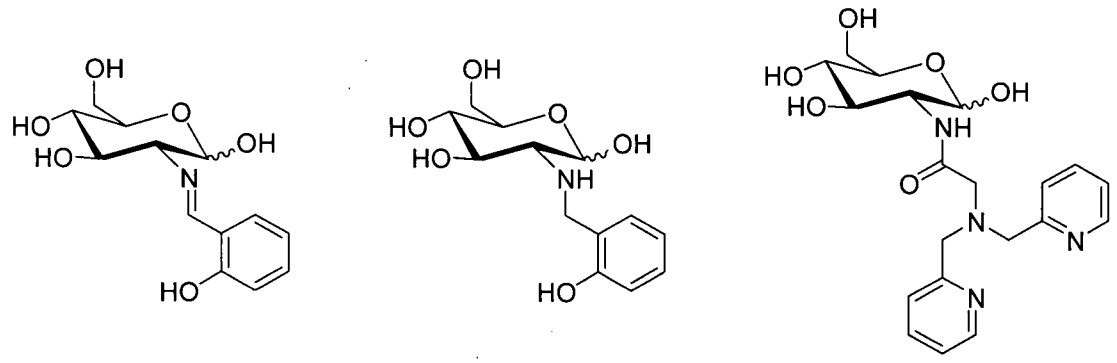

Figure 1-6. Pro-ligand progression for this project in our lab

Recent investigations in our lab have shown that a pendant glucosamine-tridentate ligand (L = 2,2'-picolylamine) **21** bound with an amide bond to the amino group of glucosamine is much more stable to challenge experiments.[13] This is despite the fact that the overall metal complex is cationic. This is supported by the synthesis and investigation of three glucose-appended 2,2'-picolylamine tridentate ligands.[15] The bidentate vs. tridentate stability issue is also seen with a series of bidentate carbohydrate-appended ligands that showed decomposition in the presence of excess cysteine and histidine, while the tridentate ligands showed excellent stability.[14]

In this thesis project, the synthesis of a glucosamine-appended tridentate pro-ligand (H**L2**), a Re complex (Re(**L2**)$(CO)_3$), and a ^{99m}Tc complex (^{99m}Tc(**L1**)$(CO)_3$) were accomplished (Figure 1-7).

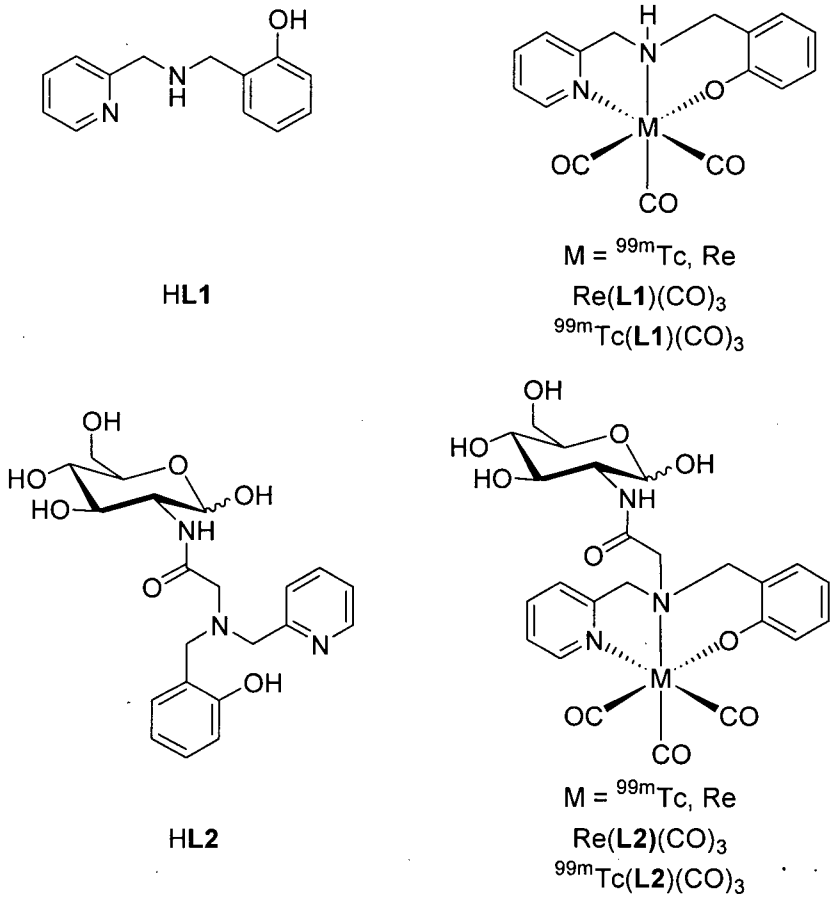

Figure 1-7. Pro-ligands and complexes made and investigated in this thesis project

The synthesis of H**L2** was investigated by two different routes, route 1 (Scheme 1-2) and route 2 (Scheme 1-3). Route 1 involved making the tridentate binding group first and then making an amide bond to the glucosamine moiety. Difficulties arising from hydrolysis resulted in an unsuccessful synthesis and led to the investigation of route 2.

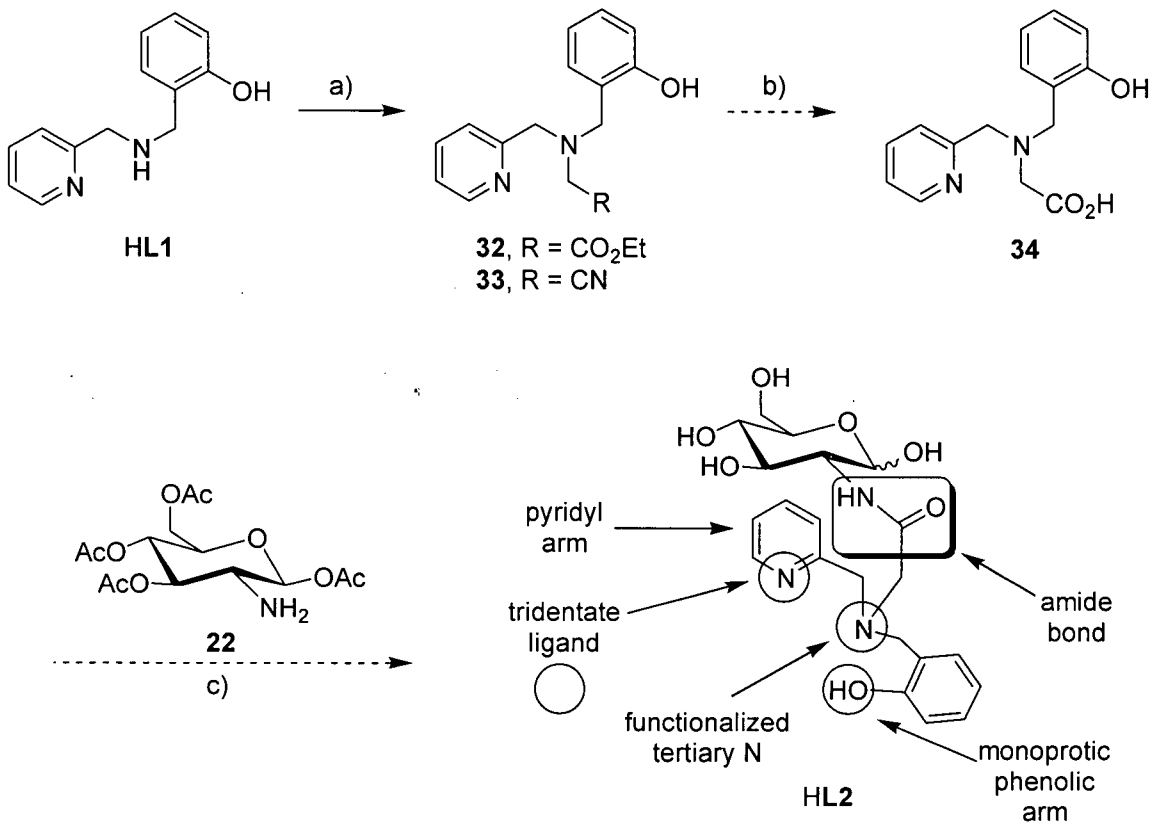

Scheme 1-2. Synthesis of H**L2** via route 1: a) ethyl bromoacetate or bromoacetonitrile, Na_2CO_3, solvent: CH_2Cl_2; b) HCl or NaOH or TFA; c) EDC.HCl, HOBt.H_2O, DMAP

Route 2 involved making 1,3,4,6-tetra-*O*-acetyl-β-*D*-glucosamine **22** and dibenzylglycine **23** from literature procedures (*vide infra*),[67, 68] reacting them together to create the spacer arm, and then systematically functionalizing the deprotected tertiary amine group to create a tridentate scaffold. This synthesis produced the desired pro-ligand H**L2** and the rhenium complex Re(**L2**)$(CO)_3$ in moderate yields.

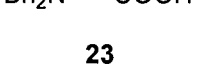

23

Furthermore, pro-ligand H**L1**, which has been synthesized previously,[69] was used to synthesize the Re complex (Re(**L2**)$(CO)_3$) to investigate binding interactions. Both ^{99m}Tc complexes (^{99m}Tc(**L1**)$(CO)_3$ and ^{99m}Tc(**L2**)$(CO)_3$) were synthesized to investigate potential *in vitro* utility.

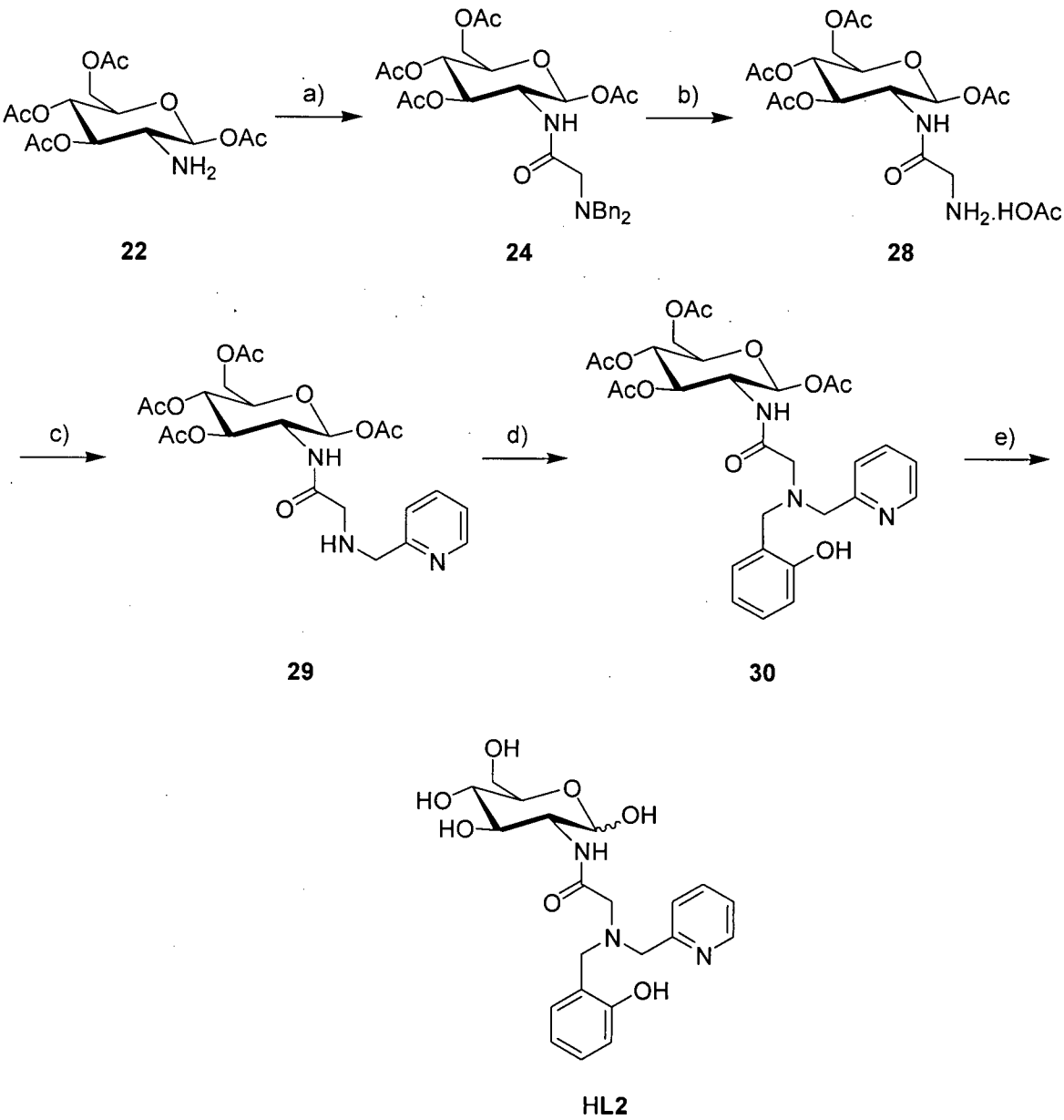

Scheme 1-3. Synthesis of H**L2** via route 2: a) **23**, EDC.HCl, HOBt.H_2O, DMAP, solvent: DMF; b) $Pd(OH)_2/C$, H_2 gas, solvent: AcOH, 18 h; c) i) 2-pca, Na_2CO_3, solvent: dichloroethane, 18 h ii) $NaBH(OAc)_3$, 4 h; d) sal, $NaBH(OAc)_3$, solvent: dichloroethane, 20 h; e) NaOMe, MeOH, 2 h

CHAPTER 2: EXPERIMENTAL

2.1 General

Except where noted otherwise, all reactions and manipulations were carried out at room temperature in reaction flasks that were flushed with Ar before use. All solvents were used as received from Aldrich or Sigma, except dry dichloromethane, which was refluxed over CaH_2 and then distilled under Ar. All compounds were reagent grade, and used as received from Sigma, Aldrich, or Fluka. *N,N*-Dibenzylglycine[67] and 1,3,4,6-tetra-O-acetyl-β-D-glucosamine.HCl[68] were synthesized according to literature procedures with a few modifications to the syntheses (these will be discussed in Chapter 3). 2-(((2-Pyridylmethyl)amino)methyl)phenol[69] (**HL1**) was synthesized according to literature procedures. All NMR (nuclear magnetic resonance) spectra were acquired in deuterated solvents (purchased from Cambridge Isotope Labs) at room temperature in the UBC Chemistry NMR facility on a Bruker Avance 300 spectrometer (300 MHz), a Bruker Avance 400 spectrometer (400 MHz and 100 MHz), or a Bruker Avance 600 spectrometer (600 MHz). Infrared spectra were recorded on a Nicolet 4700 FT-IR (Fourier transform infrared) spectrophotometer in transmission mode as KBr discs between 400 and 4000 cm^{-1} at a resolution of ±4 cm^{-1}. LR-MS and HR-MS (low and high resolution mass spectrometry, respectively) were obtained using ESIMS (electrospray ionization mass spectrometry) and APCI (atmospheric pressure chemical ionization), and EA (elemental analysis) were all done in the departmental facilities. Plates used for TLC (thin layer chromatography) (0.2 mm silica gel 60 F_{254} on alumina) and silica gel used for column chromatography (230-400 mesh) were purchased from Silicycle (Montreal, PQ). $[Re(CO)_3(H_2O)_3]Br$ was made from $Re(CO)_5Br$ (Strem)

according to literature procedures.[4] TLC spots were visualized under a UVG-54 Mineralight® short-wave UV lamp (λ = 254 nm). Carbohydrate-containing compounds were visualized as charring spots using TLC plates that were developed in a 5:95 sulfuric acid:ethanol mixture using a heat gun.

2.2 Compounds for synthesis of HL2 via route 1 (Scheme 3-1, page 38)

Ethyl 2-(*N*-(2-hydroxybenzyl)-*N*-((pyridin-2-yl)methyl)amino)acetate, 32. **HL1** (500 mg, 2.4 mmol) was dissolved in 30 mL CH_2Cl_2, Na_2CO_3 (750 mg, 7.1 mmol) was added, and the mixture cooled in an ice-water bath. Ethyl bromoacetate (260 μL, 2.4 mmol) was added slowly over 5 minutes. The solution was stirred under an Ar purge (~1 bubble per second through an oil bubbler) for 48 h after allowing warming to room temperature. The reaction mixture was filtered and the filtrate was reduced to an oily residue. The residue was purified via silica gel column chromatography (dissolve in minimal amount of CH_2Cl_2 and then elute with EtOAc) to give a yellow oil **32** (550 mg, 78% yield). R_f = 0.54 (EtOAc). ^{1}H NMR (DMSO-d_6, 300 MHz, 25°C, δ): 10.01 (s, 1H), 8.51 (d, J = 4.8 Hz, 1H), 7.79 (td, J = 7.5 and 1.7 Hz, 1H), 7.41 (d, J = 7.9 Hz, 1H), 7.29 (m, 1H), 7.11 (m, 2H), 6.77 (m, 2H), 4.09 (q, J = 7.1 Hz, 2H), 3.92 (s, 2H), 3.79 (s, 2H), 3.37 (s, 2H), 1.18 (t, J = 7.1 Hz, 3H). LR-MS (ES+): *m/z* 301 (MH^+, 100%), 323 (MNa^+, 45%).

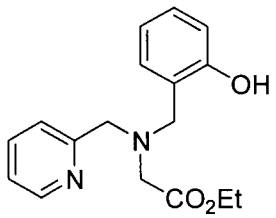

32

2-(*N*-(2-Hydroxybenzyl)-*N*-((pyridin-2-yl)methyl)amino)acetonitrile, 33. **HL1** (1.5 g, 7.1 mmol) was dissolved in 50 mL CH_2Cl_2, Na_2CO_3 (4.5 g, 42 mmol) was added, and the mixture cooled in an ice-water bath. Bromoacetonitrile (500 μL, 7.1 mmol) was added

slowly over 5 minutes. The solution was stirred under an Ar purge (~1 bubble per second through an oil bubbler) for 48 h after allowing warming to room temperature. The compound was purified via silica gel column chromatography (5%MeOH:CH_2Cl_2) to give a red oil **33** (1.3 g, 70% yield). R_f = 0.63 (10%MeOH:CH_2Cl_2). ^{1}H NMR (DMSO-d_6, 300 MHz, 25°C, δ): 9.84 (br s, 1H), 8.53 (d, J = 0.90 Hz, 1H), 7.81 (td, J = 5.9 and 1.5 Hz, 1H), 7.46 (d, J = 5.9 Hz, 1H), 7.32 (m, 1H), 7.21 (dd, J = 5.7 and 1.3 Hz, 1H), 7.12 (td, J = 5.7 and 1.3 Hz, 1H), 6.82 (dd, J = 6.1 and 0.7 Hz, 1H), 6.78 (dd, J = 5.5 and 0.8 Hz, 1H), 3.87 (s, 2H), 3.69 (s, 2H), 3.64 (s, 2H). LR-MS (ES+): *m/z* 254 (MH^+, 100%), 276 (MNa^+, 75%).

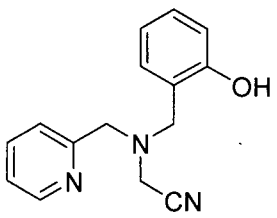

33

2-(*N*-(2-Hydroxybenzyl)-*N*-((pyridin-2-yl)methyl)ammine)tricarbonylrhenium(I), Re(L1)(CO)$_3$. HL1 (24 mg, 0.11 mmol) was dissolved in 1 mL EtOH. NaOEt (39 mg, 5.1 mmol) was added and the suspension stirred for 1h at room temperature. $[Re(CO)_3(H_2O)_3]Br$ (50 mg, 0.12 mmol) was added and the reaction mixture stirred overnight at reflux. Following consumption of the starting material by TLC (silica gel, 5%MeOH:CH_2Cl_2) and mass spectrometry, the solvent was removed under reduced pressure yielding a white solid. The solid was purified via silica gel chromatography (5%MeOH:CH_2Cl_2 eluent) to yield a white solid Re(**L1**)(CO)$_3$ (33 mg, 60% yield). R_f = 0.45 (10%MeOH:CH_2Cl_2). ^{1}H NMR (MeOH-d_4, 400 MHz, 25°C, δ): 8.63 (d, J = 5.3 Hz, 1H), 7.60 (td, J = 7.8 and 1.5 Hz, 1H), 7.15 (t, J = 6.6 Hz, 1H), 7.07 (d, J = 7.8 Hz, 1H), 7.00 (bs, 1H), 6.82 (dd, J = 7.4 and 1.4 Hz, 1H), 6.75 (td, J = 7.8 and 1.6 Hz, 1H), 6.34 (td, J = 7.3 and 0.92 Hz, 1H), 6.20 (d, J = 8.0 Hz, 1H), 4.35 (m,

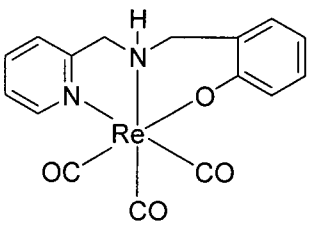

Re(**L1**)(CO)$_3$

2H), 4.03 (dd, J = 11.9 and 2.0 Hz, 1H), 3.73 (dd, J = 11.9 and 3.6 Hz, 1H). ^{13}C NMR (MeOH-d_4, 100.63 MHz, 25°C, δ): 199.2, 198.9, 197.0, 163.4, 162.5, 153.1, 140.3, 131.4, 131.0, 125.4, 124.9, 122.6, 120.7, 117.6, 60.4, 54.5. IR (KBr) ν_{max} (cm^{-1}): 2203 (s), 1909 (s), 1887 (s), 1610 (w), 1458 (m), 759 (m), 647 (w), 630 (w), 530 (w) cm^{-1}. LR-MS (AP+): *m/z* 483 ($M^{185}ReH^+$, 50%), 485 ($M^{187}ReH^+$, 100%). HR-MS (ES+ of MH^+): calcd for $C_{16}H_{14}N_2O_4{}^{187}Re$ 485.0511, found 485.0509. Anal. Calcd. for $C_{16}H_{13}N_2O_4Re.H_2O$: C, 38.32; H, 3.01; N, 5.59. Found: C, 37.87; H, 2.85; N, 5.61.

2.3 Compounds for synthesis of HL2 via route 2 (Scheme 3-3, page 42)

2-((Bis(phenylmethyl)amino)acetamido)-2-deoxy-1,3,4,6-tetra-*O*-acetyl-β-*D*-glucopyranose, 24. *N*,*N*-Dibenzylglycine (5.00 g, 0.0196 mol) was dissolved in hot DMF (125 mL). The resulting clear colourless solution was cooled in an ice bath. EDC.HCl (*N*-(3-dimethylaminopropyl)-*N*′-ethylcarbodiimide hydrochloride) (4.14 g, 0.0216 mol), HOBt.H_2O (1-hydroxybenzotriazole hydrate) (2.92 g, 0.0216 mol), and DMAP (4-dimethylaminopyridine) (0.239 g, 0.00196 mol) were added sequentially to the DMF solution. The reaction mixture was stirred at 0°C for 30 minutes and to this solution was added 1,3,4,6-tetra-*O*-acetyl-β-D-glucosamine (6.81 g, 0.0196 mol). The ice-bath was removed and the clear colourless solution was stirred overnight for 18 h after warming to room temperature. Following consumption of the starting material as monitored by TLC (silica-5%MeOH:CH_2Cl_2), the solvent was removed under reduced pressure, leaving behind a pale white solid. The solid was

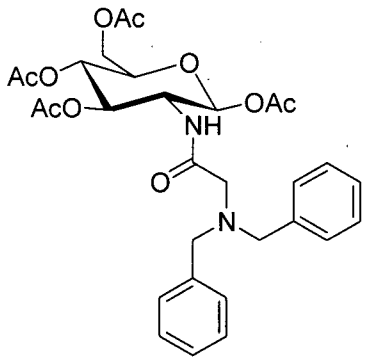

24

dissolved in 125 mL CH_2Cl_2 and 125 mL saturated aqueous Na_2CO_3 solution was added. The mixture was partitioned in a 500 mL separatory funnel and the aqueous layer was removed. The organic layer was washed with 1M HCl (125 mL) and then washed with brine (125 mL). The organic layer was removed from the separatory funnel, dried over anhydrous $MgSO_4$, and filtered through a glass frit. The filtrate was reduced to dryness under reduced pressure. The solid was purified via column chromatography (silica-5%MeOH:CH_2Cl_2) to isolate a white solid **24** (9.25 g, 80% yield). R_f = 0.56 (5% MeOH:CH_2Cl_2). ^{1}H NMR (DMSO-d_6, 400 MHz, 25°C, δ): 7.97 (d, J = 9.6 Hz, 1H), 7.29 (m, 10H), 5.99 (d, J = 8.4 Hz, 1H), 5.50 (t, J = 9.6 Hz, 1H), 4.91 (t, J = 10.0 Hz, 1H), 4.21 (dd, J = 12.4, 4.4 Hz, 1H), 4.04 (m, 3H), 3.53 (s, 4H), 2.93 (d, J = 16.0 Hz, 1H), 2.83 (d, J = 15.6 Hz, 1H) , 2.00 (d, J = 12.8 Hz, 6H), 1.80 (d, J = 14.0 Hz, 6H). ^{13}C NMR (DMSO-d_6, 100 MHz, 25°C, δ): 170.2, 170.0, 169.4, 169.3, 168.6, 137.7, 128.8, 128.2, 127.1, 91.7, 72.0, 71.5, 68.3, 61.5, 57.2, 55.8, 51.7, 20.5, 20.4, 20.3, 20.2. IR (KBr) ν_{max} (cm^{-1}): 1742 (s), 1663 (m), 1514 (m), 1371 (w), 1261 (m), 1225 (s), 1079 (m), 1039 (m), 740 (w). LR-MS (ES+): *m/z* 607 (MNa^+, 100%), 585 (MH^+, 20%). HR-MS (ES+ of MNa^+): calcd for $C_{30}H_{36}N_2O_{10}Na$ 607.2268, found 607.2267. Anal. Calcd. for $C_{30}H_{36}N_2O_{10}$: C, 61.63; H, 6.21; N, 4.79. Found: C, 61.90; H, 6.59; N, 5.11.

2-(((*N-tert*-Butoxycarbonyl)amino)acetamido)-2-deoxy-1,3,4,6-tetra-*O*-acetyl-β-*D*-glucopyranose, 25. BOC-Gly-OH (1.01 g, 5.77 mmol) was dissolved in 30 mL CH_2Cl_2 and the solution cooled in an ice-water bath. To this solution, DCC (dicyclohexylcarbodiimide) (1.31 g, 6.35 mmol), HOBt (1-hydroxybenzotriazole) (0.858 g, 6.35 mmol) and DMAP (0.070 g, 0.58 mmol) were added sequentially and the resulting solution stirred for 18 h after warming to room temperature. The suspension

was filtered to remove dicyclohexylurea, and 1,3,4,6-tetra-O-acetyl-β-D-glucosamine.HCl (2.21 g, 5.77 mmol) and triethylamine (0.89 mL, 6.4 mmol) were added. The solution was stirred for an additional 18 h. The solvent was removed under reduced pressure and the residue was purified via silica gel column chromatography with 10%EtOAc:MeOH as eluent to yield a white solid **25** (1.89 g, 65% yield). R_f = 0.60 (10%EtOAc:MeOH). ^{1}H NMR ($CDCl_3$, 300 MHz, 25°C, δ): 6.82 (br d, J = 8.3 Hz, 1H), 5.73 (d, J = 8.7 Hz, 1H), 5.36 (br s, 1H), 5.24 (t, J = 9.3 Hz, 1H), 5.05 (t, J = 9.7 Hz, 1H), 4.21 (dd, J = 12.5 and 4.7 Hz, 2H), 4.05 (dd, J = 12.5 and 2.1 Hz, 1H), 3.83 (br dd, J = 6.5 and 2.0 Hz, 1H), 3.62 (d, J = 5.8 Hz, 2H), 2.00 (m, 12H), 1.36 (s, 9H). LR-MS (ES+): *m/z* 505 (MH^+, 100%), 527 (MNa^+, 30%).

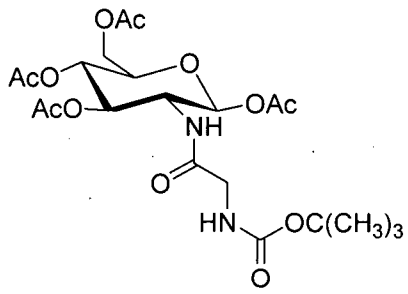

25

2-(((*N*-9-Fluorenylmethoxycarbonyl)amino)acetamido)-2-deoxy-1,3,4,6-tetra-*O*-acetyl-β-*D*-glucopyranose, 26. FMOC-Gly-OH (301 mg, 1.01 mmol) was dissolved in 6 mL DMF and 6 mL CH_2Cl_2 and the resulting solution was cooled in an ice-water bath. To this solution, DCC (229 mg, 1.11 mmol) and HOBt (150 mg, 1.11 mmol) were added sequentially. The reaction mixture was stirred for 2.5 h at which time 1,3,4,6-tetra-O-acetyl-β-D-glucosamine (351 mg, 1.01 mmol) was added and the reaction mixture was stirred for 16 h total. The reaction mixture was filtered to remove dicyclohexylurea, the solvent was removed under reduced pressure, and the residue was purified via silica gel column chromatography (dissolved in minimal

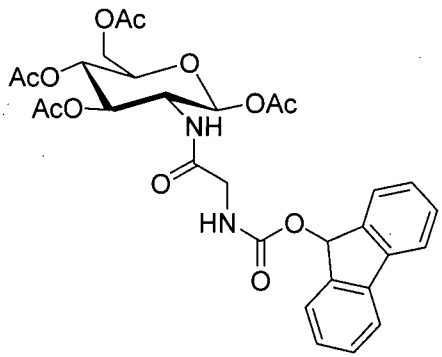

26

amount of CH_2Cl_2 and eluted with EtOAc) to yield a pale white solid **26** (380 mg, 60% yield). R_f = 0.60 (EtOAc). ^{1}H NMR ($CDCl_3$, 400 MHz, 25°C, δ): 7.74 (d, J = 7.6 Hz, 2H), 7.56 (d, J = 7.2 Hz, 2H), 7.38 (t, J = 7.6 Hz, 2H), 7.27 (m, 2H), 6.56 (br d, J = 8.8 Hz, 1H), 5.75 (d, J = 8.8, 1H), 5.50 (s, 1H), 5.21 (t, J = 9.6 Hz, 1H), 5.10 (t, J = 9.6 Hz, 1H), 4.39 (dd, J = 17.6 and 10.4 Hz, 2H), 4.22 (m, 3H), 4.09 (m, 1H), 3.80 (m, 1H), 3.73 (d, J = 5.6 Hz, 2H), 2.06 (s, 6H), 2.01 (s, 6H). LR-MS (ES+): *m/z* 627 (MH^+, 100%), 649 (MNa^+, 20%).

2-(((*N*-Benzyloxycarbonyl)amino)acetamido)-2-deoxy-1,3,4,6-tetra-*O*-acetyl-β-D-glucopyranose, 27. CBZ-Gly-OH (2.10 g, 10.0 mmol) was dissolved in 50 mL DMF and the solution cooled in an ice-water bath. To this solution, DCC (2.27 g, 11.0 mmol), HOBt (1.49 g, 11.0 mmol) and DMAP (0.122 g, 1.0 mmol) were added sequentially and the resulting solution stirred for 1 h. To this solution, 1,3,4,6-tetra-O-acetyl-β-D-glucosamine (3.47 g, 10.0 mmol) was added. The reaction mixture was stirred for an additional 17 h at room temperature. The solvent was removed under reduced pressure and the residue was purified via silica gel column chromatography with 5%MeOH:CH_2Cl_2 eluent to yield a pale white solid **27** (3.23 g, 60% yield). R_f = 0.54 (5%MeOH:CH_2Cl_2). ^{1}H NMR (DMSO-d_6, 400 MHz, 25°C, δ): 7.90 (d, J = 9.6 Hz, 1H), 7.49 (t, J = 6.0 Hz, 1H), 7.34 (m, 5H), 5.75 (d, J = 8.8 Hz, 1H), 5.23 (t, J = 9.6 Hz, 1H), 5.01 (s, 2H), 4.88 (t, J = 10.0 Hz, 1H), 4.19 (dd, J = 12.8 and 4.8 Hz, 1H), 4.00 (m, 3H), 3.51 (d, J = 6.0 Hz, 2H), 1.92 (m, 12H). LR-MS (ES+): *m/z* 539 (MH^+, 40%), 561 (MNa^+, 100%).

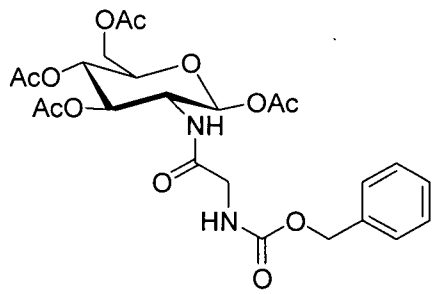

27

2-(2-Aminoacetamido)-2-deoxy-1,3,4,6-tetra-*O*-acetyl-β-*D*-glucopyranosyl acetate 28. Compound **24** (7.64 g, 0.0131 mol) was dissolved in 100 mL acetic acid. $Pd(OH)_2/C$ (0.800 g, 0.0057 mmol) was added in one portion and the flask was capped with a rubber septum and purged with H_2 from a balloon. The mixture was kept under a positive pressure of H_2 from the H_2-balloon overnight for 18 h. The absence of starting material was confirmed by TLC (silica-5%MeOH:CH_2Cl_2) and mass spectrometry. The suspension was filtered through a celite plug (~ 1cm in a small frit) giving a clear pale yellow solution. The solvent was removed under reduced pressure to yield a yellow oil **28** (6.08 g, 100%). R_f = 0.05 (5%MeOH:CH_2Cl_2). ^{1}H NMR (DMSO-d_6, 400 MHz, 25°C, δ): 5.76 (d, J = 8.8 Hz, 1H), 5.22 (t, J = 10.0 Hz, 1H), 4.90 (t, J = 10.0 Hz, 1H), 4.19 (dd, J = 12.4 and 4.4 Hz, 1H), 4.01 (m, 3H), 3.39 (s, 2H), 2.03 (m, 12H). ^{13}C NMR (DMSO-d^6, 100 MHz, 25°C, δ) 172.6, 170.2, 169.9, 169.8, 169.4, 169.0, 91.7, 72.1, 71.6, 68.2, 61.6, 52.2, 41.1, 21.5, 20.6, 20.6, 20.5, 20.4. LR-MS (AP–): *m/z* 403 ((M-HOAc), 50%), 463 (M^-, 100%). HR-MS (ES– of M^-) calcd for $C_{18}H_{27}N_2O_{12}$ 463.1564, found 463.1567. *Note:* IR was not obtained due to decomposition and EA was not obtained due to varying amounts of acetic acid present in the oily sample.

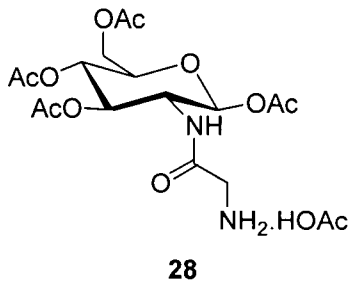

28

2-(((*N*-Pyridin-2-ylmethyl)amino)acetamido)-2-deoxy-1,3,4,6-tetra-*O*-acetyl-β-*D*-glucopyranose, 29. Compound **28** (9.80 g, 0.0104 mol) was dissolved in 100 mL dichloroethane. Na_2CO_3 (34.2 g, 0.323 mol) and 2-pyridinecarboxaldehyde (0.989 mL, 0.0104 mol) were added sequentially. The cloudy red solution was stirred overnight for 18 h. $NaBH(OAc)_3$ (6.85 g, 0.0323 mol) was added in one portion after consumption of

the starting material was confirmed by TLC and mass spectrometry, and the reaction mixture was stirred for an additional 4 h. The white solid was removed via filtration through a glass frit. The resulting clear orange solution was concentrated under reduced pressure to give a yellow solid. The yellow solid was dissolved in 50 mL CH_2Cl_2 and the solution was added to a separatory funnel, followed by addition of 50 mL saturated aqueous Na_2CO_3. The aqueous layer was removed and the organic layer was washed with brine. The organic layer was dried over anhydrous $MgSO_4$ and reduced to a yellow solid. The solid was purified via column chromatography (silica-5%MeOH:CH_2Cl_2 eluent) to give a pale yellow solid **29** (2.19 g, 43% yield). R_f = 0.51 (10%MeOH:CH_2Cl_2). ^{1}H NMR (DMSO-d_6, 400 MHz, 25°C, δ): 8.49 (d, J = 7.8 Hz, 1H), 8.09 (d, J = 9.7 Hz, 1H), 7.75 (t, J = 7.5 Hz, 1H), 7.39 (d, J = 7.8 Hz, 1H), 7.25 (t, J = 5.8 Hz, 1H), 5.89 (d, J = 8.8 Hz, 1H), 5.37 (t, J = 9.6 Hz, 1H), 4.90 (t, J = 9.6 Hz, 1H), 4.19 (dd, J = 12.4 and 4.4 Hz, 1H), 4.01 (m, 3H), 3.65 (s, 2H), 3.09 (s, 2H), 1.97 (m, 12H). ^{13}C NMR (DMSO-d_6, 100 MHz, 25°C, δ): 171.4, 170.1, 169.7, 169.3, 168.9, 159.4, 148.8, 136.5, 122.1, 121.9, 91.9, 72.2, 71.5, 68.2, 61.5, 53.9, 51.7, 51.5, 20.6, 20.5, 20.4, 20.4. IR (KBr) ν_{max} (cm^{-1}): 1747 (s), 1668 (m), 1522 (m), 1371 (w), 1229 (s), 1074 (m), 1041 (m), 598 (w). LR-MS (ES+): *m/z* 496 (MH^+, 100%), 518 (MNa^+, 30%). HR-MS (ES+ of MH^+): calcd for $C_{22}H_{30}N_3O_{10}$ 496.1931, found 496.1930. Anal. Calcd. for $C_{22}H_{29}N_3O_{10}$: C, 53.33; H, 5.90; N, 8.48. Found: C, 53.41; H, 6.20; N, 8.65.

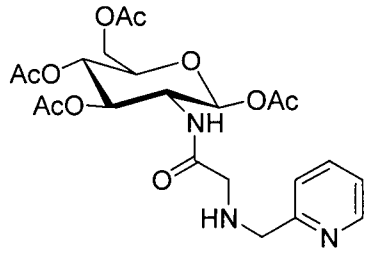

29

2-((*N*-(2-Hydroxybenzyl)-*N*-(pyridin-2-ylmethyl)amino)acetamido)-2-deoxy-1,3,4,6-tetra-*O*-acetyl-β-*D*-glucopyranose, 30. Compound **29** (700 mg, 1.4 mmol) was dissolved in 15 mL dichloroethane. Salicylaldehyde (470 μL, 4.4 mmol) and $NaBH(OAc)_3$ (1.5 g, 7.2 mmol) were added sequentially and the reaction mixture was stirred overnight for 20 h. Following consumption of the starting material as confirmed by TLC (silica-10%MeOH:CH_2Cl_2) and mass spectrometry, the reaction mixture was reduced to dryness under reduced pressure. The residue was dissolved in 25 mL CH_2Cl_2 and 25 mL saturated aqueous Na_2CO_3 solution and 25 mL water were added and the suspension partitioned in a separatory funnel. The aqueous layer was removed and the organic layer was washed with brine. The organic layer was dried over anhydrous $MgSO_4$, filtered, and the solvent removed under reduced pressure to give a yellow solid. The solid was purified using column chromatography (silica-5%MeOH:CH_2Cl_2 eluent) to give a yellow solid **30** (0.670 g, 79% yield). R_f = 0.74 (10%MeOH:CH_2Cl_2). ^{1}H NMR (DMSO-d_6, 400 MHz, 25°C, δ): 9.95 (s, 1H), 8.50 (d, J = 2.4 Hz, 2H), 7.72 (td, J = 7.8 and 1.8 Hz, 1H), 7.35 (d, J = 7.6 Hz, 1H), 7.27 (t, J = 6.6 Hz, 1H), 7.13 (m, 2H), 6.77 (m, 2H), 5.86 (d, J = 8.8 Hz, 1H), 5.35 (t, J = 9.6 Hz, 1H), 4.92 (t, J = 9.8 Hz, 1H), 4.21 (dd, J = 12.4 and 4.6 Hz, 1H), 4.04 (m, 3H), 3.66 (s, 2H), 3.59 (s, 2H), 3.07 (d, J = 16.6 Hz, 2H), 3.00 (d, J = 16.6 Hz, 2H), 2.01 (s, 3H), 1.98 (s, 3H), 1.92 (s, 3H), 1.83 (s, 3H). ^{13}C NMR (DMSO-d_6, 100 MHz, 25°C, δ): 170.5, 170.0, 169.5, 169.3, 168.7, 158.2, 156.2, 148.8, 136.7, 130.8, 128.6, 123.1, 122.5, 122.3, 118.8, 115.4, 91.6, 72.0, 71.5, 68.1, 61.5, 58.2, 56.0, 53.7, 51.8, 20.5, 20.4, 20.4, 20.2. IR (KBr) $\nu_{max.}$ (cm^{-1}): 3314 (m), 1754 (s), 1685 (m), 1522

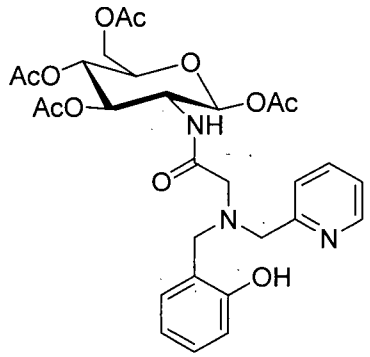

30

(w), 1368 (m), 1221 (s), 1078 (m), 1040 (m), 760 (m) cm^{-1}. LR-MS (ES+): *m/z* 602 (MH^+, 100%), 624 (MNa^+, 40%). HR-MS (ES+ of MH^+): calcd for $C_{29}H_{36}N_3O_{11}$ 602.2350, found 602.2348. Anal. Calcd. for $C_{29}H_{35}N_3O_{11}$: C, 57.90; H, 5.86; N, 6.98. Found: C, 58.04; H, 6.28; N, 7.29.

2-((*N*-(2-Hydroxybenzyl)-*N*-(pyridin-2-ylmethyl)amino)acetamido)-2-deoxy-*D*-glucopyranose, H**L2.** Compound **30** (670 mg, 1.11 mmol) was dissolved in 5 mL MeOH. NaOMe (310 mg, 5.7 mmol) was added in one portion and the solution stirred for 2 h. Following consumption of the starting material by TLC (silica-20%MeOH:CH_2Cl_2) and mass spectrometry, the solvent was removed under reduced pressure to yield a pale white solid. The solid was purified using silica gel chromatography with 20%MeOH:CH_2Cl_2 as the eluent to yield a pale yellow solid H**L2** (300 mg, 62% yield). R_f = 0.34 (20%MeOH:CH_2Cl_2). ^{1}H NMR (MeOH-d_4, 400 MHz, 25°C, δ): 8.48 (m, 1H), 7.77 (m, 1H), 7.51 (m, 1H), 7.28 (m, 1H), 7.12 (m, 2H), 6.79 (m, 2H), 5.06 (d, J = 3.5 Hz, 1H-β), 4.64 (d, 8.4 Hz, 1H-α), 3.78 (m, 9H), 3.35 (m, 1H), 3.23 (s, 2H). ^{13}C NMR (MeOH-d_4, 100 MHz, 25°C, δ): 174.5, 159.7, 158.0, 149.6, 139.0, 132.3, 130.3, 124.9, 124.5, 124.0, 120.5, 117.1, 97.1 (α), 92.7 (β), 73.2, 73.0, 72.6, 63.0, 60.2, 58.0, 56.7, 55.8. IR (KBr) ν_{max} (cm^{-1}): 3386 (br, s), 1655 (s), 1597 (w), 1541 (w), 1489 (w), 1247 (m), 1104 (w), 1039 (m), 758 (s) cm^{-1}. LR-MS (ES+): *m/z* 434 (MH^+, 100%), 456 (MNa^+, 30%). HR-MS (ES+ of MH^+): calcd for $C_{21}H_{28}N_3O_7$ 434.1927, found 434.1925. Anal. Calcd. for $C_{21}H_{27}N_3O_7$.(0.6 H_2O): C, 56.77; H, 6.40; N, 9.46. Found: C, 56.52; H, 6.23; N, 9.21.

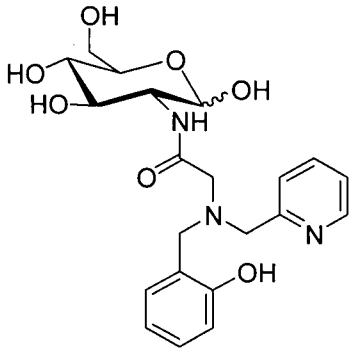

HL2

2-(((*N*-(2-Hydroxybenzyl)-*N*-(pyridin-2-ylmethyl)amino)acetamido)-2-deoxy-*D*-glucopyranosyl)tricarbonylrhenium(I), Re(L2)(CO)$_3$. HL**2** (40 mg, 0.092 mmol) was dissolved in 2 mL MeOH. [Re(CO)$_3$(H$_2$O)$_3$]Br (41 mg, 0.10 mmol) was added in one portion and the reaction mixture stirred for 2h at reflux. Following consumption of the starting material by TLC (20%MeOH:CH_2Cl_2) and mass spectrometry, the solvent was removed under reduced pressure leaving a pale orange solid. The solid was purified via silica gel column chromatography (20%MeOH:CH_2Cl_2 eluent) resulting in a pale white solid Re(**L2**)(CO)$_3$ (47 mg, 72% yield). R_f = 0.27 (20%MeOH:CH_2Cl_2). ^{1}H NMR (MeOH-d_4, 400 MHz, 25°C, δ): 8.85 (m, 1H), 8.07 (m, 1H), 7.70 (m, 1H), 7.53 (m, 2H), 7.35 (t, J = 8.3 Hz, 1H), 7.00 (dd, J = 8.0 and 2.8 Hz, 2H), 5.01 (m, 4H), 4.87 (d, J = 3.6 Hz, 1H), 4.62 (d, J = 9.1 Hz, 1H), 4.43 (m, 1H), 3.71 (m, 5H), 3.25 (m, 2H). ^{13}C NMR (MeOH-d_4, 100 MHz, 25°C, δ): 197.5, 196.8, 182.3, 160.7, 158.0, 154.1, 142.5, 134.9, 132.7, 127.3, 125.4, 121.2, 119.7, 117.3, 95.8, 91.8, 73.1, 72.0, 71.9, 69.1, 68.1, 63.0, 62.6. IR (KBr) ν_{max} (cm^{-1}): 3386 (br, m), 2032 (s), 1905 (s), 1618 (m), 1458 (w), 764 (w). LR-MS (ES+): *m/z* 702 ($M^{185}ReH^+$, 50%), 704 ($M^{187}ReH^+$, 100%). HR-MS (ES+ of MH^+): calcd for $C_{24}H_{27}N_3O_{10}{}^{187}Re$ 704.1254, found 704.1256.

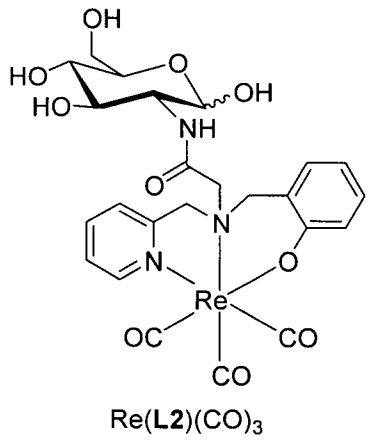

Re(**L2**)(CO)$_3$

2-(((*N*-*tert*-Butoxycarbonyl)-*N*-(pyridin-2-ylmethyl)amino)acetamido)-2-deoxy-1,3,4,6-tetra-*O*-acetyl-β-*D*-glucopyranose, 31. Compound **29** (260 mg, 0.525 mmol) was dissolved in 5 mL CH_2Cl_2. Na_2CO_3 (1.4 g, 13 mmol) and *tert*-butyl bromoacetate

(700 μL, 1.3 mmol) were added sequentially and the reaction mixture stirred under a slow Ar purge (~1 bubble per second through an oil bubbler) for 48 h. Following consumption of the starting material by TLC (silica-10%MeOH:CH_2Cl_2) and mass spectrometry, the reaction mixture was filtered to remove a white solid. The solvent was removed under reduced pressure and the resulting yellow solid was purified via silica gel column chromatography (10%MeOH:CH_2Cl_2 eluent) to yield a pale yellow solid **31** (220 mg, 68% yield). R_f = 0.66 (10%MeOH:CH_2Cl_2). ^{1}H NMR (DMSO-d_6, 400 MHz, 25°C, δ): 8.52 (d, J = 4.0 Hz, 1H), 8.31 (d, J = 9.2 Hz, 1H), 7.74 (td, J = 7.6 and 2.0 Hz, 1H), 7.45 (d, J = 8.0 Hz, 1H), 7.28 (dd, J = 7.2 and 5.2 Hz, 1H), 5.90 (d, J = 8.8 Hz, 1H), 5.38 (t, J = 9.6 Hz, 1H), 4.90 (t, J = 10.0 Hz, 1H), 4.20 (dd, J = 12.4 and 4.4 Hz, 1H), 4.03 (m, 3H), 3.84 (s, 2H), 3.25 (s, 4H), 2.01 (s, 3H), 1.97 (s, 3H), 1.94 (s, 3H), 1.86 (s, 3H), 1.41 (s, 9H). ^{13}C NMR (DMSO-d_6, 100 MHz, 25°C, δ): 170.3, 170.0, 169.8, 169.5, 169.2, 168.7, 158.1, 149.0, 136.6, 122.8, 122.4, 91.7, 80.5, 72.1, 71.5, 68.2, 61.5, 59.1, 56.7, 54.8, 51.7, 27.8, 20.5, 20.4, 20.3, 20.2. IR (KBr) ν_{max} (cm^{-1}): 1751 (s), 1665 (m), 1517 (m), 1369 (m), 1225 (s), 1152 (w), 1074 (m), 1040 (m). LR-MS (ES+): *m/z* 610 (MH^+, 10%), 632 (MNa^+, 100%). HR-MS (ES+ of MNa^+): calcd for $C_{28}H_{39}N_3O_{12}Na$ 632.2431, found 632.2432. Anal. Calcd. for $C_{28}H_{39}N_3O_{12}$: C, 55.17; H, 6.45; N, 6.89. Found: C, 55.60; H, 6.30; N, 6.90.

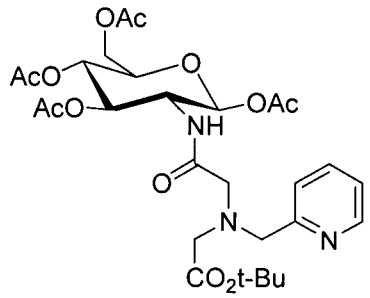

31

2.4 Preparation and characterization of ^{99m}Tc complexes

Following synthesis and characterization of Re(**L1**)$(CO)_3$ and Re(**L2**)$(CO)_3$, the following procedure was used to make the corresponding ^{99m}Tc-complexes,

^{99m}Tc(**L1**)(CO)$_3$ and ^{99m}Tc(**L2**)(CO)$_3$. To make the [^{99m}Tc(CO)$_3$(H$_2$O)$_3$]$^+$ precursor, Na[^{99m}TcO$_4$] (0.07 mL, 150 MBq) was diluted to 1 mL with saline (0.154 M NaCl, 0.9%), added to an Isolink™ kit, and the resulting reaction vial was heated to 100°C for 20 min. Following a brief cooling period, 1M HCl (~ 0.12 mL) was added to adjust the pH to around 9-10. The ligand solutions were made as follows: a 1 mM solution of H**L1** (2.4 mg, 0.010 mmol) or H**L2** (4.3 mg, 0.010 mmol) in 10 mL EtOH was prepared and a solution of NaOEt (8.8 mg, 0.13 mmol) in 10 mL EtOH was prepared. To 1 mL of ethanolic NaOEt in a 5 mL reaction vial, 1 mL of H**L1** or H**L2** in EtOH was added and the resulting solutions were left for 10 minutes at room temperature. To each of these solutions, 0.5 mL of the [^{99m}Tc(CO)$_3$(H$_2$O)$_3$]$^+$ solution was added, and the resulting solutions were heated to 70°C for 30 min. The identities of the radiolabelled complexes were confirmed to be ^{99m}Tc(**L1**)(CO)$_3$ and ^{99m}Tc(**L2**)(CO)$_3$, following HPLC co-injection with the corresponding Re complexes, Re(**L1**)(CO)$_3$ and Re(**L2**)(CO)$_3$, respectively. The HPLC apparatus used was a Knauer Wellchrom K-1001 with a K-2501 absorption detector at λ = 254 nm. A Synergi 4 μm C-18 Hydro-RP analytical column (250mm x 4.6 mm) was used with HPLC solvent consisting of 0.1 % w/w TFA in water (solvent A) and MeOH (solvent C). Corresponding HPLC traces are shown in Chapter 3 (*vide infra*).

2.5 Cysteine and histidine challenge experiments

Cysteine and histidine challenge experiments were used to test the *in vitro* stability of ^{99m}Tc(**L1**)(CO)$_3$ and ^{99m}Tc(**L2**)(CO)$_3$. Following synthesis of [^{99m}Tc(CO)$_3$(H$_2$O)$_3$]$^+$ and preparation of the ligand solutions (*vide infra*), 0.1 mL of the Isolink™ kit solution (*i.e.* containing either ^{99m}Tc(**L1**)(CO)$_3$ and ^{99m}Tc(**L2**)(CO)$_3$) was added to one 5 mL reaction vial (radiolabelling control), to each of three 5 mL reaction

vials containing 0.9 mL of 1 mM cysteine in PBS buffer (pH 7.4, cysteine challenge experiment), and to each of three 5 mL reaction vials containing 1 mL of 1 mM histidine in PBS buffer (pH 7.4, histidine challenge experiment). A cloudy solution developed in each of the cysteine and histidine reaction vials. The challenge experiments were performed at 4 and 24 h time-points at room temperature. HPLC analysis was performed by co-injecting 5 μL of (Re(**L1**)$(CO)_3$ or Re(**L2**)$(CO)_3$) with 10 μL of ^{99m}Tc(**L1**)$(CO)_3$ and ^{99m}Tc(**L2**)$(CO)_3$, respectively. The complexes were eluted with a fixed solvent method over 30 minutes (40%A:60%C for ^{99m}Tc(**L2**)$(CO)_3$; 15%A:85%C for ^{99m}Tc(**L1**)$(CO)_3$). Corresponding HPLC traces are shown in Chapter 3 (*vide infra*).

CHAPTER 3: RESULTS AND DISCUSSION

3.1 Design and synthesis of tridentate glucosamine complexes

The design and synthesis of tridentate glucosamine complexes can be accomplished using either linear or convergent syntheses. Previous methodology from our laboratories utilized linear syntheses,[12-15] and it was thought that this would be more efficient in designing a tunable tridentate binding unit; *i.e.* varying the dibenzylglycine methylene lengths or changing the tridentate functionality. Two syntheses were envisioned, where the first route (route 1, Scheme 3-1, page 38) would involve making the tridentate binding unit first, followed by coupling to the glucosamine moiety, and the second route (route 2, Scheme 3-3, page 42) would involve making the spacer arm first, followed by further functionalization to produce the desired binding site. Investigations into both syntheses showed the second route to be the preferred method. However, the starting material for the first route (*i.e.* H**L1**) led to the synthesis of Re(**L1**)$(CO)_3$ that was used to model the binding of the ligand to the metal centre.

3.2 Retrosynthetic analysis and synthesis of HL2 (route 1)

Shown in Figure 3-1 is the retrosynthetic analysis of H**L2** via route 1. This route emphasized the synthesis of **35** via N-alkylation of H**L1**, deprotection, and amide coupling to **22**. Investigations focused on the synthesis of the tridentate binding unit, which would then lead to the attachment of the binding moiety to a glucosamine molecule **22** via an amide bond using EDC.HCl, HOBt.H_2O, and DMAP (Scheme 3-1).[70-72] Several attempts were made to synthesize the tripodal binding unit **34**, consisting of a pyridyl arm, a monoprotic phenolic arm, and a functionalized tertiary N atom. The

synthesis began with the starting material H**L1** according to literature procedures.[69] This was followed by N-alkylation with either ethyl bromoacetate to make **32** or bromoacetonitrile to make **33**, in the presence of excess Na_2CO_3 in CH_2Cl_2 to create two tridentate precursors.[59, 73]

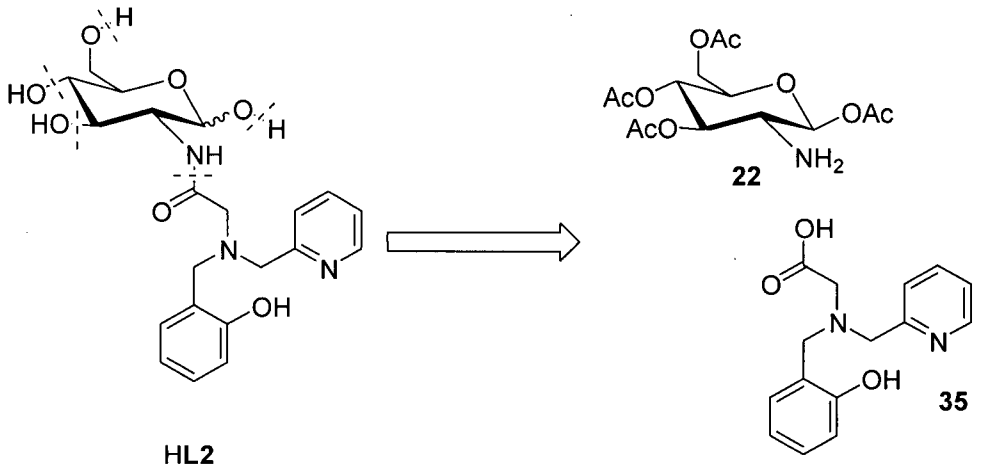

Figure 3-1. Retrosynthetic analysis of H**L2** via route 1

The first attempt to remove the ethyl ester and the cyano moieties used acid hydrolysis. However neither 1M HCl nor concentrated HCl at room temperature and reflux resulted in isolation of **34** as either a free acid or salt after workup; this was despite mass spectrometry evidence of **34** as a free acid (ES+, *m/z* = 273 (M+1)) or salt. The second attempt involved using base hydrolysis to obtain **34**. Likewise, the use of 1M NaOH or 12M NaOH (at room temperature and reflux) did not afford isolation of **34** despite evidence by mass spectrometry (ES–, *m/z* = 271 (M–1)). Unfortunately, no tridentate product **34** (as a free acid or salt) was obtained with a free carboxylate arm, and therefore, no attempts at amide coupling with **22** to make H**L2** were undertaken. Such difficulties prompted the investigation of synthesis via route 2 for H**L2**.

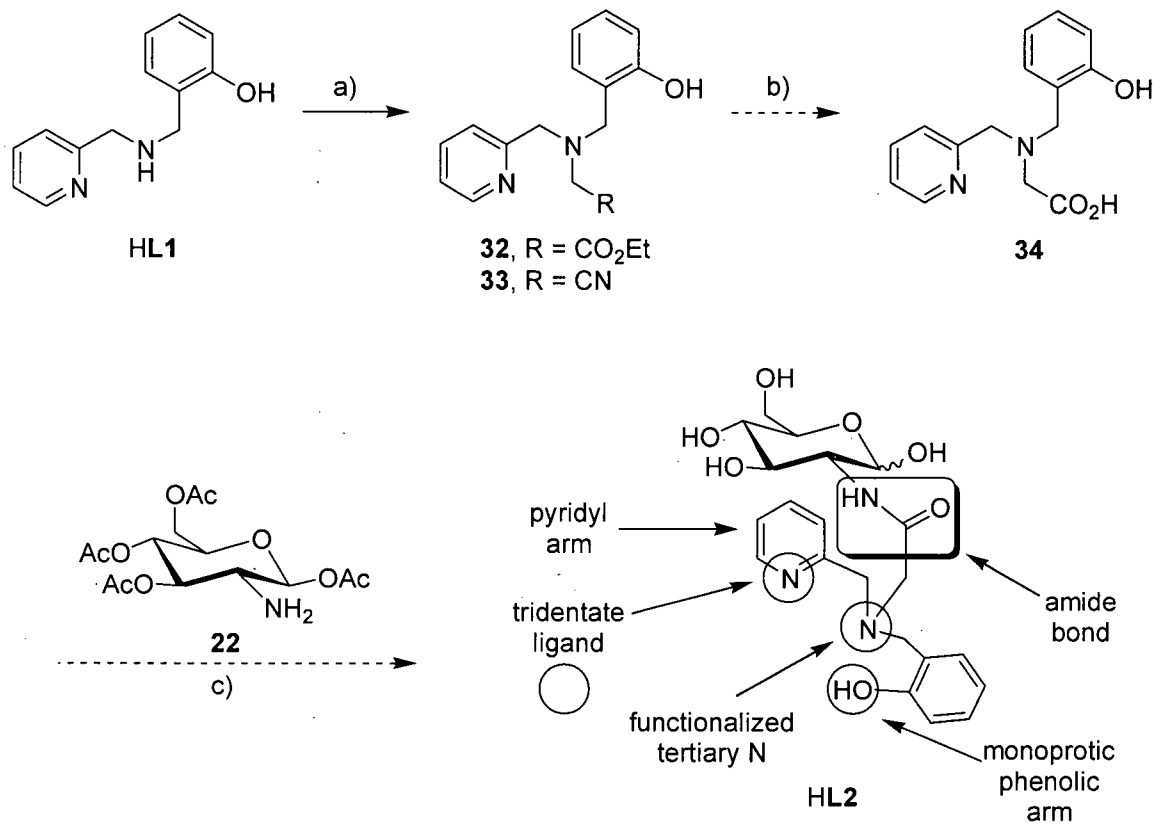

Scheme 3-1. Synthesis of HL**2** via route 1: a) ethyl bromoacetate or bromoacetonitrile, Na_2CO_3, solvent: CH_2Cl_2; b) HCl or NaOH or TFA; c) EDC.HCl, HOBt.H_2O, DMAP

3.3 Retrosynthetic analysis of 24 and synthesis of 22 and 23

Before undertaking route 2, compound **24** first was required. This compound was chosen over **25**, **26**, and **27** because the deprotection was quantitative and occurred without any side-product formation. As indicated by retrosynthetic analysis (Figure 3-2), the synthesis of **24** would require the synthesis of two compounds, 1,3,4,6-tetra-*O*-acetyl-β-*D*-glucosamine **22** and dibenzylglycine **23**, from literature procedures (Scheme 3-2).[67, 68] These would be combined using an amide coupling reaction.[70-72]

1,3,4,6-Tetra-*O*-acetyl-β-*D*-glucosamine **22** and dibenzylglycine **23** (Scheme 3-2) were made from literature procedures with a few modifications.[67, 68] For the synthesis of

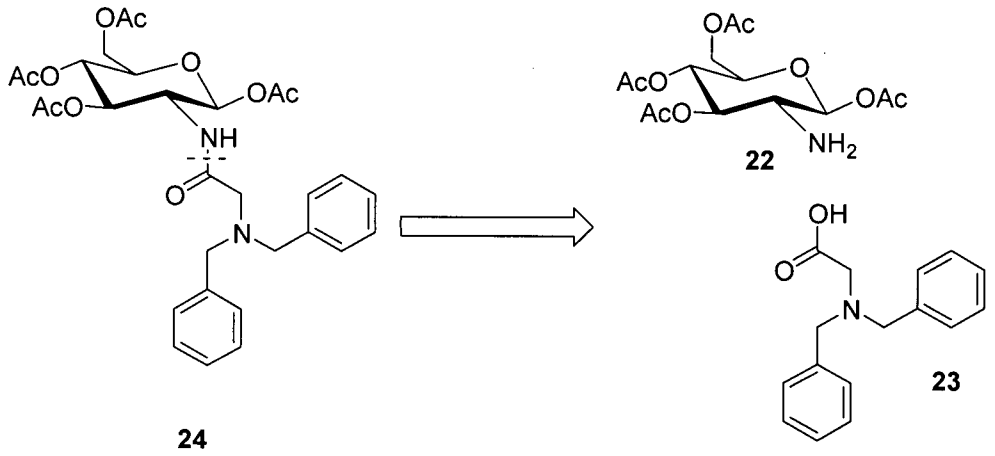

Figure 3-2. Retrosynthetic analysis of **24**

1,3,4,6-tetra-*O*-acetyl-β-*D*-glucosamine **22**, compound **37** was made quantitatively from β-*D*-glucosamine.HCl **36** by first synthesizing the free base of **36** with aqueous NaOH and then protecting the amine with *p*-anisaldehyde. Compound **38** was obtained in very good yield following acetylation of **37** with acetic anhydride in the presence of excess pyridine and a catalytic amount of DMF. The amine salt **39** was isolated as a gelatinous mass following acidification of **38** with 5M HCl from a hot solution of acetone. To improve the purity and yield of **39**, a few extra steps were undertaken. Upon repeated washings with copious amounts of Et_2O, stirring, and filtering, the product **39** was obtained as a white powder. If not enough Et_2O was added (it dissolves the liberated *p*-anisaldehyde), then contamination with **36** and/or with *p*-anisaldehyde resulted (as detected by ^1H NMR spectroscopy). This inevitably led to further product contamination with byproducts and lower yields further along in the synthesis. Free base **22** was obtained from **39** nearly quantitatively by slurrying **39** in saturated aqueous Na_2CO_3 and extraction into CH_2Cl_2. In addition, **39** can be stored on the bench top with little decomposition, whereas **22** decomposes quite readily.

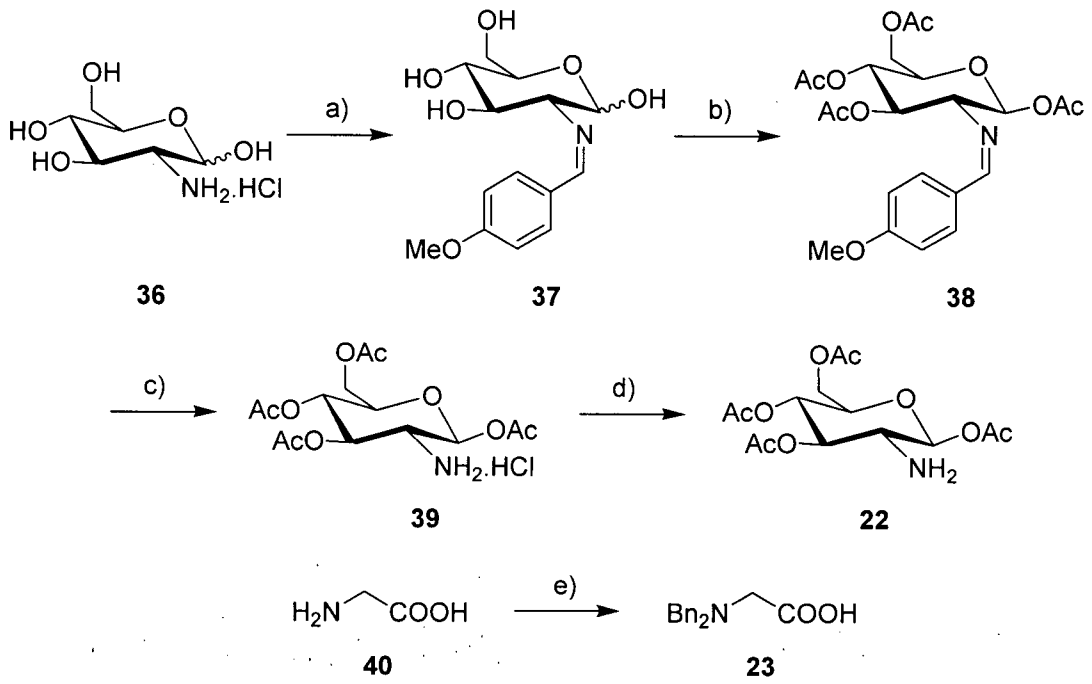

Scheme 3-2. Precursor synthesis conditions: a) *p*-anisaldehyde, 1M NaOH; b) Ac_2O, pyridine, DMAP; c) 5M HCl, acetone; d) Saturated aqueous Na_2CO_3, CH_2Cl_2; e) i) BnBr, 1M NaOH ii) AcOH to ~ pH 6

For the synthesis of dibenzylglycine **23**, a basic solution of glycine **40** in water was placed in an ice-water bath. Benzyl bromide (BnBr) was added dropwise to the cold solution and the reaction mixture was stirred overnight (precipitation of **23** is almost immediate). The mixture was decreased to half-volume under reduced pressure and then acidified to pH ~6 with acetic acid (AcOH). The precipitate was collected via filtration in very good yields. Further to the literature procedure and to increase the purity and yield, a slurry of **23** in 1:1 EtOH:H_2O was heated to reflux and stirring continued for a few minutes. Compound **23** was obtained as white powder, without any acetic acid impurity (as evidenced by ^{1}H NMR spectroscopy), following filtration and air drying. It can also be stored on the bench top with little decomposition.

3.4 Retrosynthetic analysis and synthesis of HL2 (route 2)

The retrosynthetic analysis of **HL2** via route 2 is shown in Figure 3-3. Such a synthesis (*vide infra*) would require deprotection of the tertiary amine of **24** and subsequent functionalization with 2-pyridinecarboxaldehyde (2-pca) and salicylaldehyde (sal); this would be followed by removal of the acetyl groups with NaOMe and MeOH.

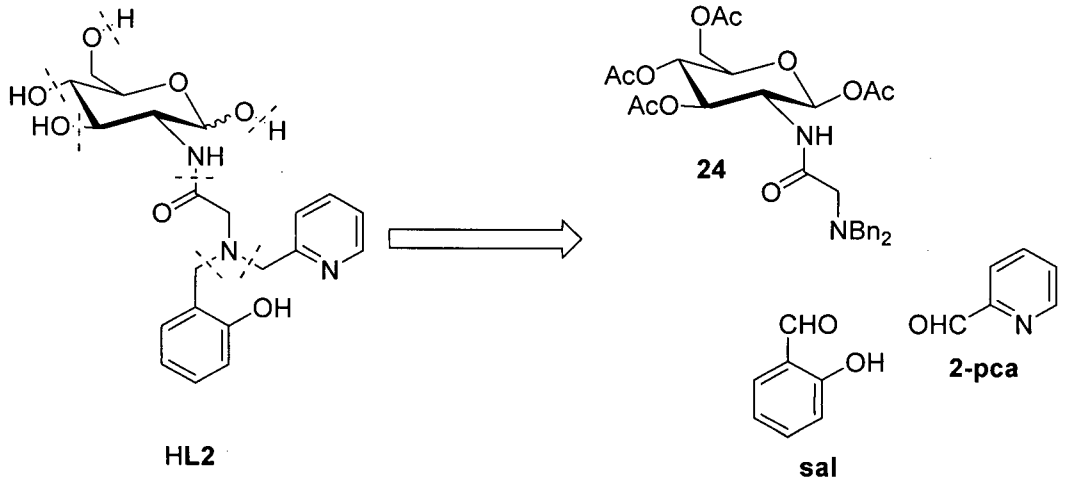

Figure 3-3. Retrosynthetic analysis of **HL2** via route 2

The synthesis of **HL2** (Scheme 3-3) began after the synthesis of compound **24**, itself formed from coupling of **22** and **23** using EDC.HCl, HOBt.H_2O, and DMAP in DMF.[70-72] THF was used initially as the solvent for the amide coupling reaction but higher yields were obtained using DMF and the addition of a small amount of DMAP improved the reaction in DMF slightly. This was followed by hydrogenolysis using Pearlman's catalyst ($Pd(OH)_2$ on C)[74, 75] in acetic acid, and isolation of **28** as the acetate salt. The pyridyl arm was installed via a Schiff base condensation reaction with 2-pyridine- carboxaldehyde in the presence of Na_2CO_3. This was followed by reduction of the imine *in situ* with excess $NaBH(OAc)_3$ to make compound **29**.[60] Installation of the

monoprotic phenolic arm via a reductive amination with salicylaldehyde in the presence of excess

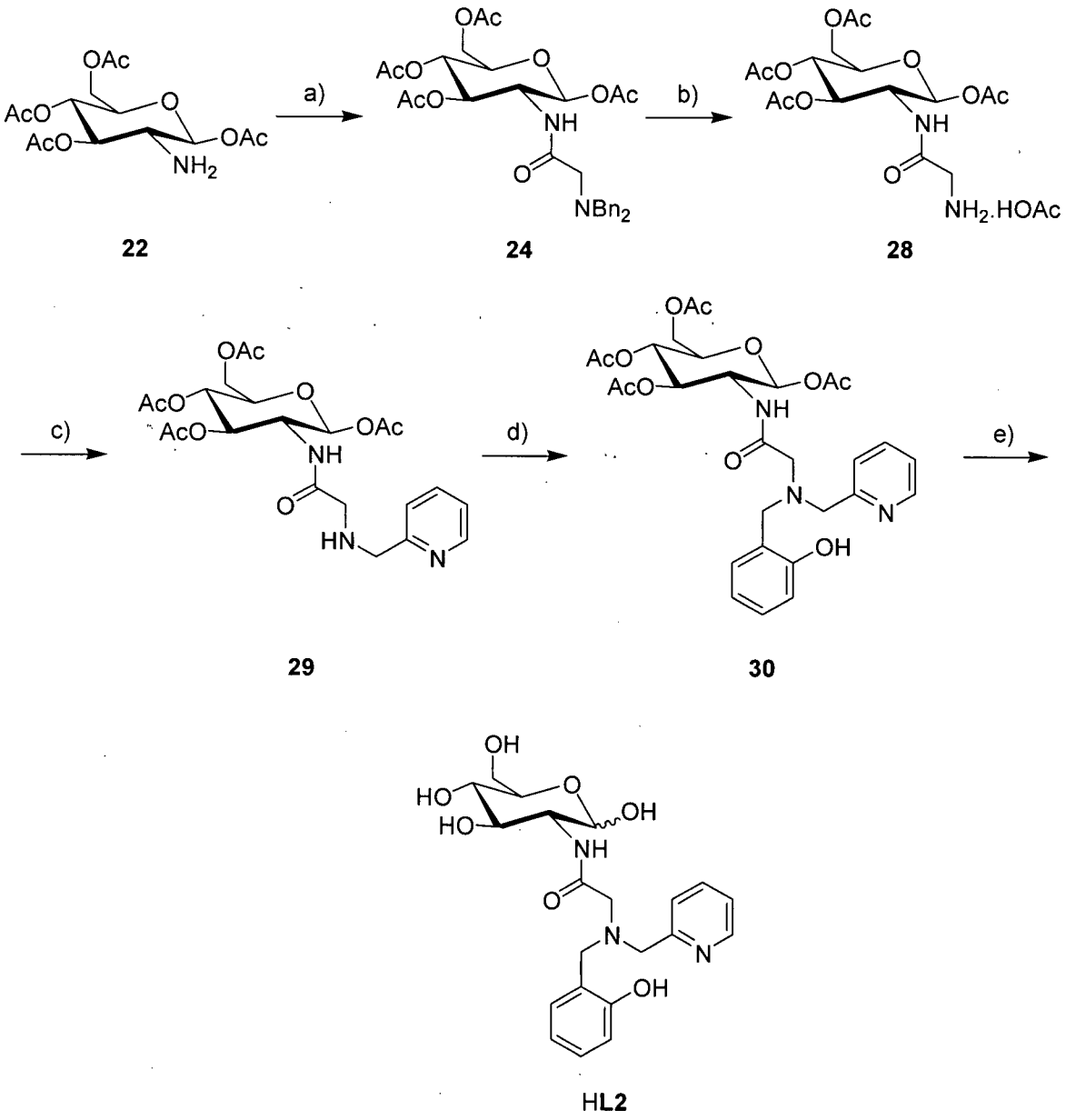

Scheme 3-3. Synthesis of H**L2** via route 2: a) **23**, EDC.HCl, HOBt.H_2O, DMAP, solvent: DMF; b) $Pd(OH)_2/C$, H_2 gas, solvent: AcOH, 18 h; c) i) 2-pca, Na_2CO_3, solvent: dichloroethane, 18 h ii) $NaBH(OAc)_3$, 4 h; d) sal, $NaBH(OAc)_3$, solvent: dichloroethane, 20 h; e) NaOMe, MeOH, 2 h

$NaBH(OAc)_3$ resulted in compound **30**.[60] The desired compound H**L2** was finally obtained following removal of the acetyl groups with NaOMe in MeOH.[76]

3.5 Synthesis and characterization of Re complexes

H**L1** and H**L2** have the same tridentate binding unit. It was thought that H**L1** could serve as a model complex for the binding of the tridentate unit and would result in 'simpler' ^1H and ^{13}C NMR spectra due to the lack of carbohydrate proton and carbon resonances. This would allow the modeling of the binding site without extraneous signals, and, hopefully, help fully assign the ^1H and ^{13}C NMR spectra of H**L2** and Re(**L2**)$(CO)_3$. The synthesis of Re-complexes Re(**L1**)$(CO)_3$ and Re(**L2**)$(CO)_3$ is shown in Scheme 3-4, and these complexes were used to investigate the binding mode of the ligands.

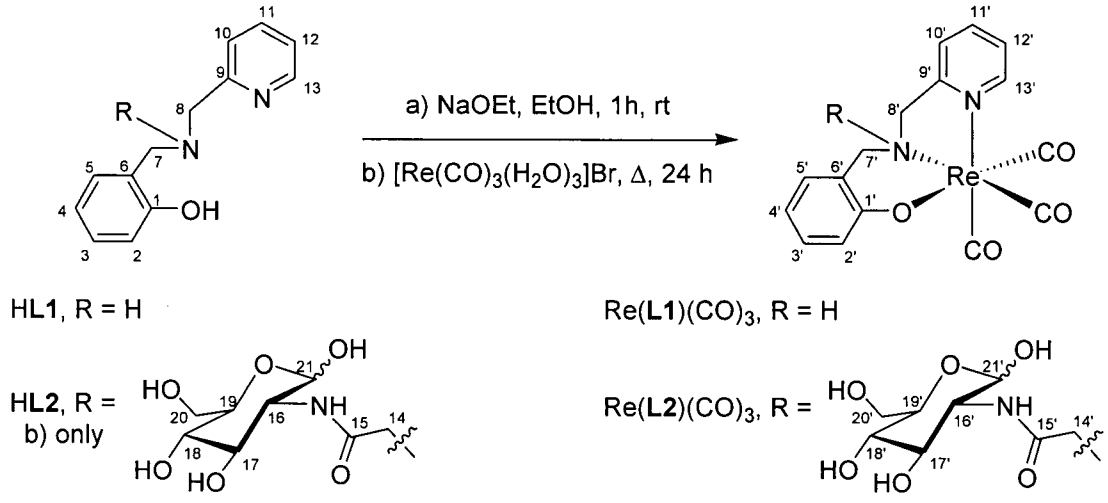

Scheme 3-4. Preparation of Re complexes

H**L1** was dissolved in EtOH, NaOEt was added, and the reaction stirred for 1 h at room temperature. $[Re(CO)_3(H_2O)_3]Br$ was added and the resulting solution stirred overnight at reflux for 24 h. H**L2** was dissolved in EtOH, $[Re(CO)_3(H_2O)_3]Br$ was

added, and the resulting solution stirred overnight at reflux for 24 h. The desired complexes were obtained as white solids following removal of the solvent and subsequent column chromatography. The complexes were characterized by ^{1}H and ^{13}C NMR spectroscopy, mass spectrometry, and IR spectroscopy. NMR spectroscopy was used to elucidate solution structures of all precursors, ligands, and Re-complexes; mass spectrometry was used to provide further evidence of the solution structures of such compounds, and IR spectroscopy was used to assign the CO stretching modes characteristic of the tricarbonyl motif.

For H**L1** and Re(**L1**)$(CO)_3$, ^{1}H and ^{13}C NMR spectra show definite shifts of the phenolic and pyridyl proton resonances. The ^{1}H NMR spectrum is shown in Figure 3-4 and the ^{13}C NMR spectrum is shown in Figure 3-5. Resonances were assigned on the basis of $^{1}H/^{1}H$ COSY (correlation spectroscopy) and $^{1}H/^{13}C$ HMQC (heteronuclear multiple quantum coherence) spectroscopy. Neither the NH proton nor the OH proton resonance of H**L1** is observed in the ^{1}H NMR spectrum; this is most likely due to proton exchange. This is not the case in the ^{1}H NMR spectrum of Re(**L1**)$(CO)_3$, where a distinct broad singlet is observed for the NH proton resonance at 7.33 ppm (NH'). Upon binding of the ligand to the metal, the NH exchange process slows compared to the NMR timescale, and the resonance for the NH signal appears in the ^{1}H NMR spectrum of Re(**L1**)$(CO)_3$. As can be seen from Figure 3-4, only the H13 resonance of the pyridine ring shifts downfield (8.52 to 8.54 ppm) while the other three pyridine aromatic resonances shift upfield: H11 (7.76 to 7.70 ppm), H12 (7.26 to 7.23 ppm), and H10 (7.41 to 7.15 ppm). This indicates binding of the pyridine nitrogen to the Re centre. For the phenolate, all four phenol aromatic resonances shift downfield: H2 (7.08 to 6.77 ppm),

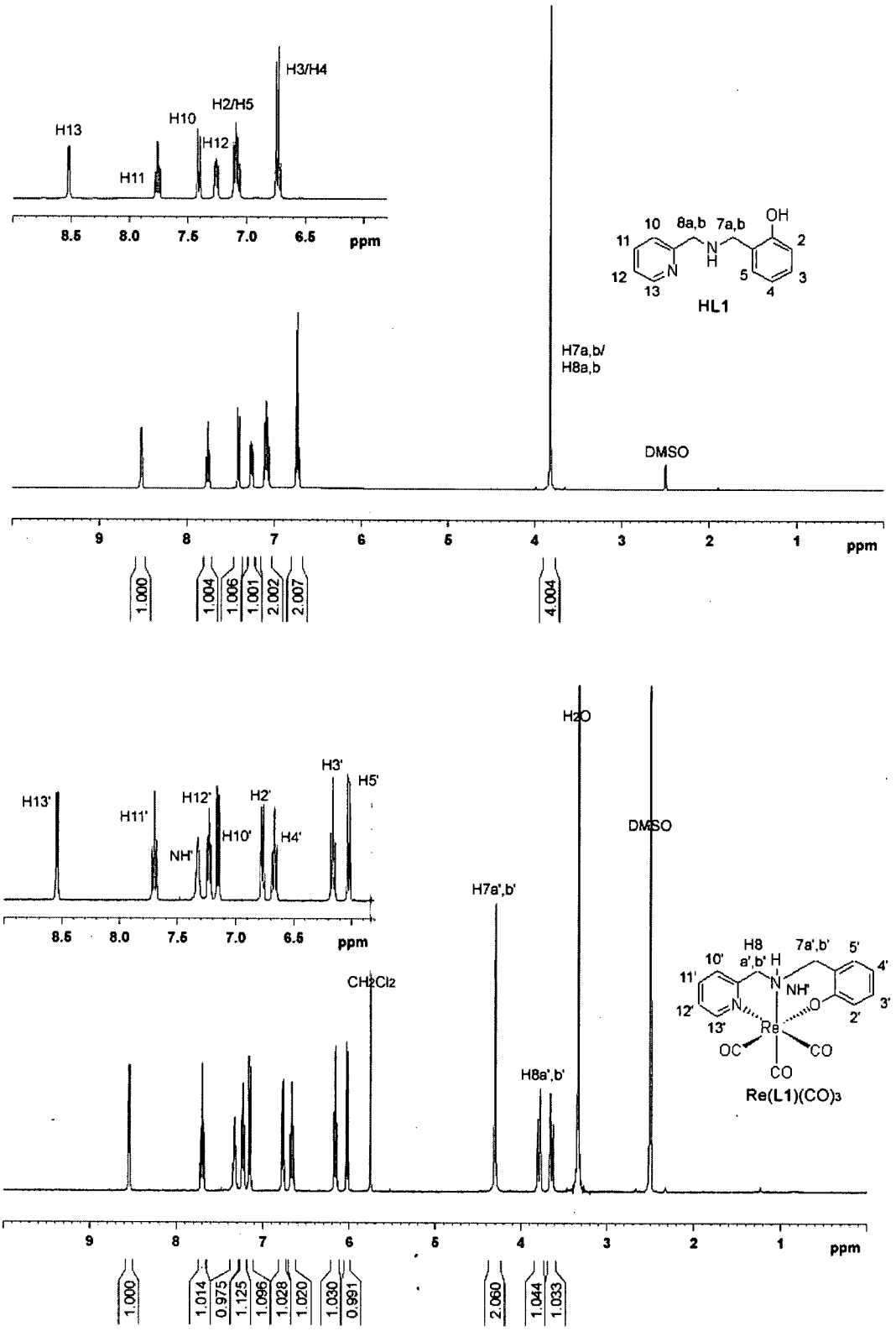

Figure 3-4. ^{1}H NMR spectra (DMSO-d_6, 400 MHz, 25°C) of H**L1** (top) and Re(**L1**)(CO)$_3$ (bottom)

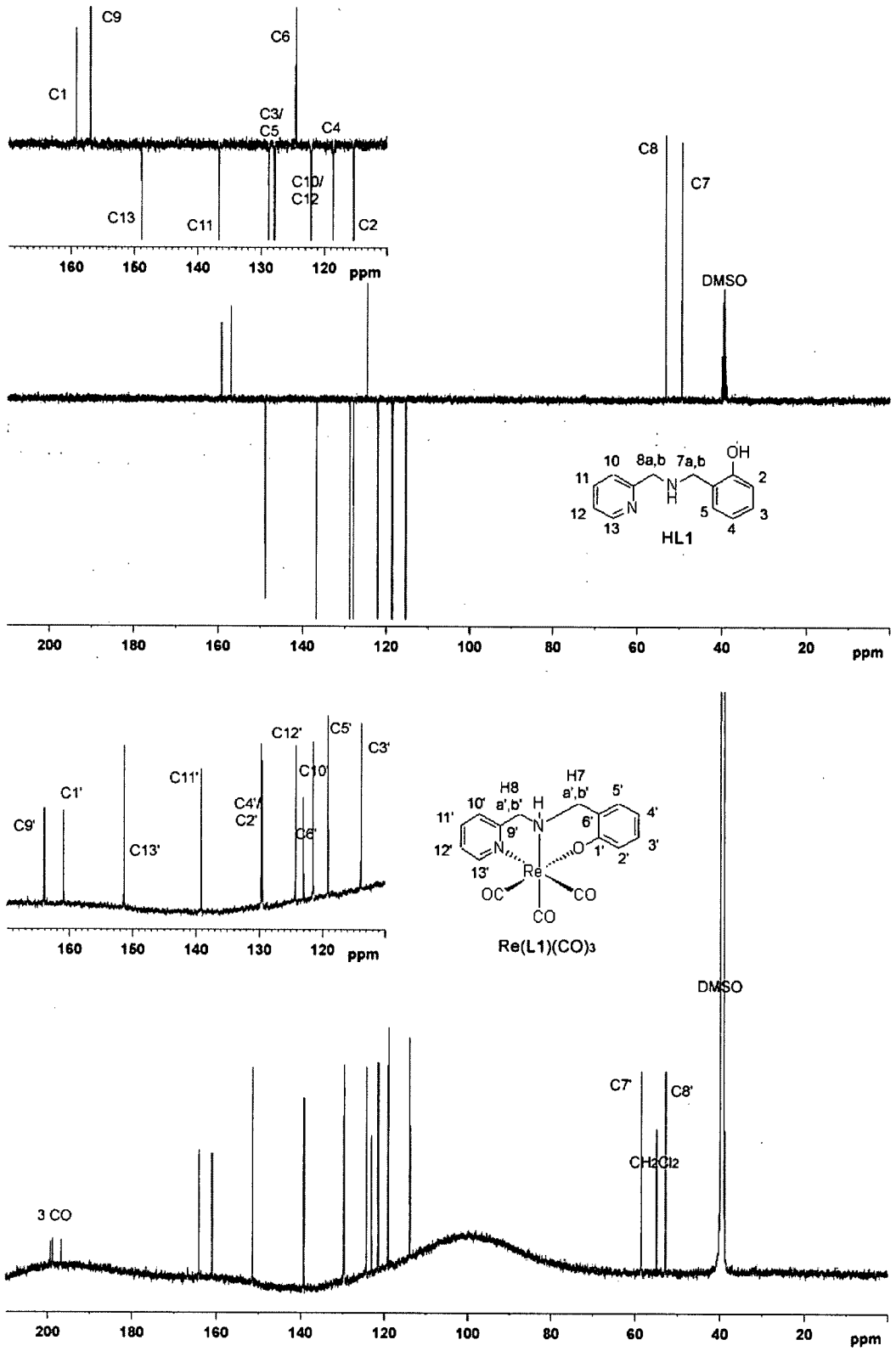

Figure 3-5. ^{13}C NMR spectra of H**L1** (top, DMSO-d_6, 100 MHz APT, 25°C) and Re(**L1**)$(CO)_3$ (bottom, DMSO-d_6, 100 MHz, 25°C)

H4 (6.73 to 6.67 ppm), H3 (6.73 to 6.16 ppm), and H5 (7.08 to 6.02 ppm). These resonance shifts indicate binding of the phenolate to the Re centre. Accompanying this evidence are the shifts and splits of the methylene resonances, H7a,b and H8a,b. In the ^{1}H NMR spectrum of H**L1**, H7a,b and H8a,b appear equivalent as one singlet at 3.82 ppm. In the ^{1}H NMR spectrum of Re(**L1**)$(CO)_3$, an upfield shift of the resonance indicates binding of the tridentate scaffold and the doublet at 4.30 ppm indicates weak coupling between H7a' and H7b'. This is not seen with H8a' and H8b', where one set of doublets of doublets is seen at 3.79 and 3.64 ppm. The coupling constant for these resonances is the same (12.0 Hz), and can be attributed to the diastereotopic nature of the CH_2 protons that occurs upon the tridentate scaffold 'locking' the conformation around the Re centre upon binding.

Such tridentate binding is further supported by the ^{13}C NMR spectrum (Figure 3-5). Upfield shifts are seen for C6' (124.5 to 123.0 ppm), C10' (122.1 to 121.5 ppm), C5' (127.9 to 119.1 ppm), and C3' (128.8 to 113.9 ppm); such large upfield shifts for these phenol resonances (C6', C5', and C3') indicate binding of the phenolate to the Re centre.Likewise, downfield shifts are seen for C9' (157.0 to 164.0 ppm), C1' (159.2 to 161.0 ppm), C13' (148.9 to 151.4 ppm), C11' (136.6 to 139.2 ppm), C4' (118.5 to 129.7 ppm), C2' (115.3 to 129.5 ppm), C12' (122.0 to 124.3 ppm). Such downfield shifts of the resonances for C13', C11', and C12' indicate binding of the pyridine to the Re centre. Effects of the tridentate binding are evident in the shifts for the resonances C7' and C8'; 49.6 to 58.6 ppm (downfield) and 53.3 to 52.8 ppm (upfield), respectively. Hence, we see that the Re centre is indeed coordinated in a tridentate fashion by the ligand.

Tridentate binding of the ligand is also evident for H**L2** and Re(**L2**)$(CO)_3$, where the ^1H (Figure 3-6) and ^{13}C (Figure 3-7) NMR spectra show similar shifts upon metal binding. The shifts due to the carbohydrate resonances were unchanged (or showed small shifts) in solution, and this helps confirm the pendant nature of the glucosamine moiety in solution. However, even with 2D NMR techniques, the corresponding spectra were quite difficult to interpret. Upon metal binding, as can be seen, the resonances due to the carbohydrate, linker, and methylene protons collapse into large multiplets. The shifts of the aromatic resonances are indicative of metal binding, however unlike for H**L1** and Re(**L1**)$(CO)_3$, the proton resonances all shift downfield: H13 (8.49 to 8.84 ppm), H11 (7.77 to 8.07 ppm), H2 (7.50 to 7.70 ppm), H10/12 (7.13 to 7.53 ppm), 4 (7.28 to 7.35 ppm), and H3/5 (6.79 to 6.99 ppm). Of note, is the appearance of the anomeric proton resonances (H21β/α) at 5.07 and 4.65 ppm, respectively, in a relative ratio of $\beta:\alpha = 2:1$.

The ^{13}C NMR spectra (Figure 3-7) are indicative of binding as well. The carbon resonances of the sugar region shift very little, indicating that the glucosamine moiety remains pendant. Interestingly, the ^{13}C NMR spectrum of the ligand and the Re complex resulted in two sets of similar, yet distinct, resonances for the carbohydrate and spacer moieties. This could be the result of either the presence of two anomers (overlaps of 2 signals) or enantiomers (overlaps of up to 4 peaks); other methods are required to deduce the correct assignment. The appearance of three carbon signals between 197.5 and 196.8 ppm in the ^{13}C NMR spectrum of Re(**L2**)$(CO)_3$ indicate an arrangement of three carbonyl groups as either the *fac* or the *mer* isomer; it is most likely the *fac* arrangement due to the tridentate nature of **L2**. Shifts of the carbon resonances from the H**L2** to the Re(**L2**)$(CO)_3$ are indicative of tridentate binding. For the aromatic resonances, C9 and

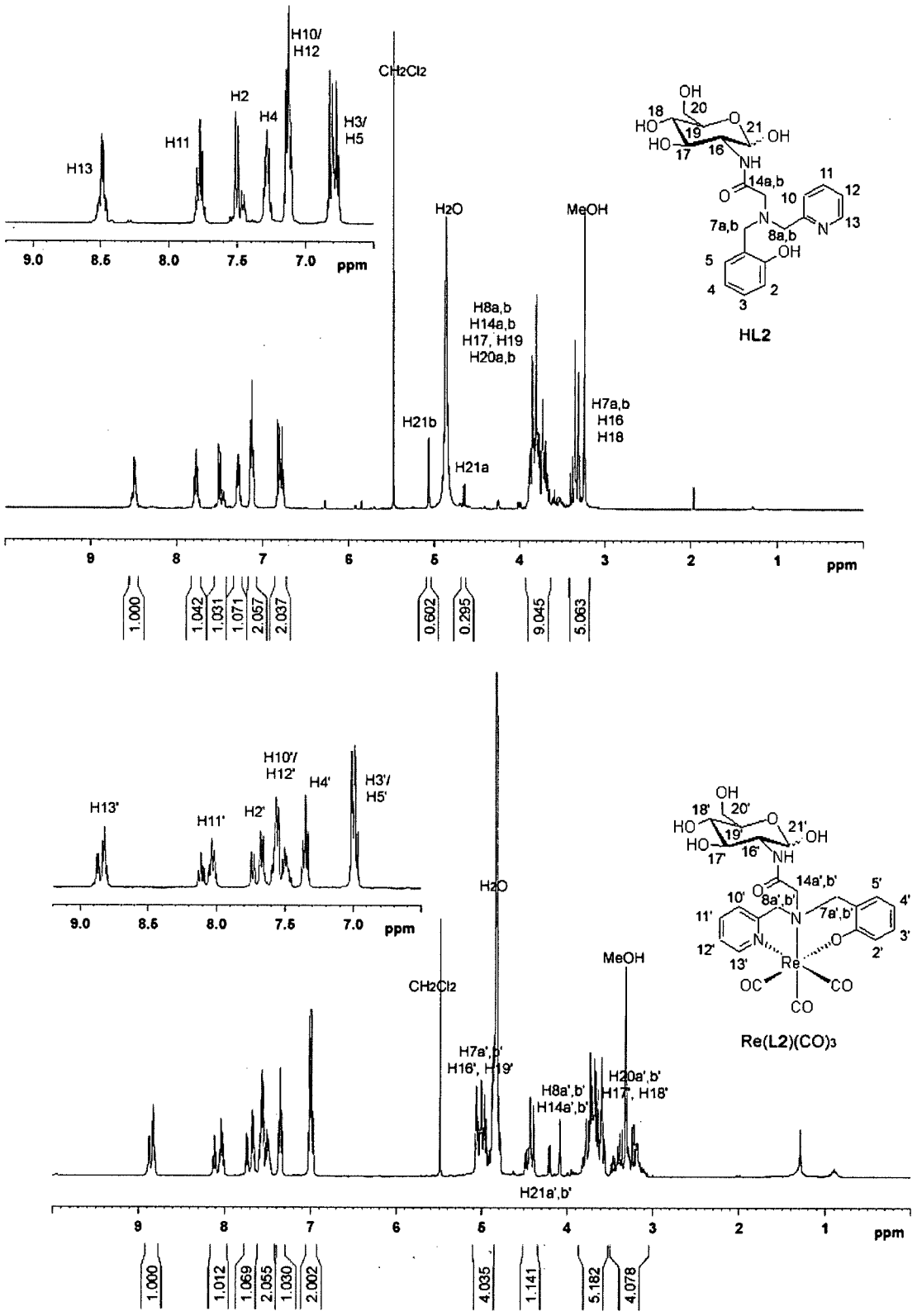

Figure 3-6. ^{1}H NMR spectra (MeOH-d_4, 400 MHz, 25°C) of H**L2** (top) and Re(**L2**)$(CO)_3$ (bottom)

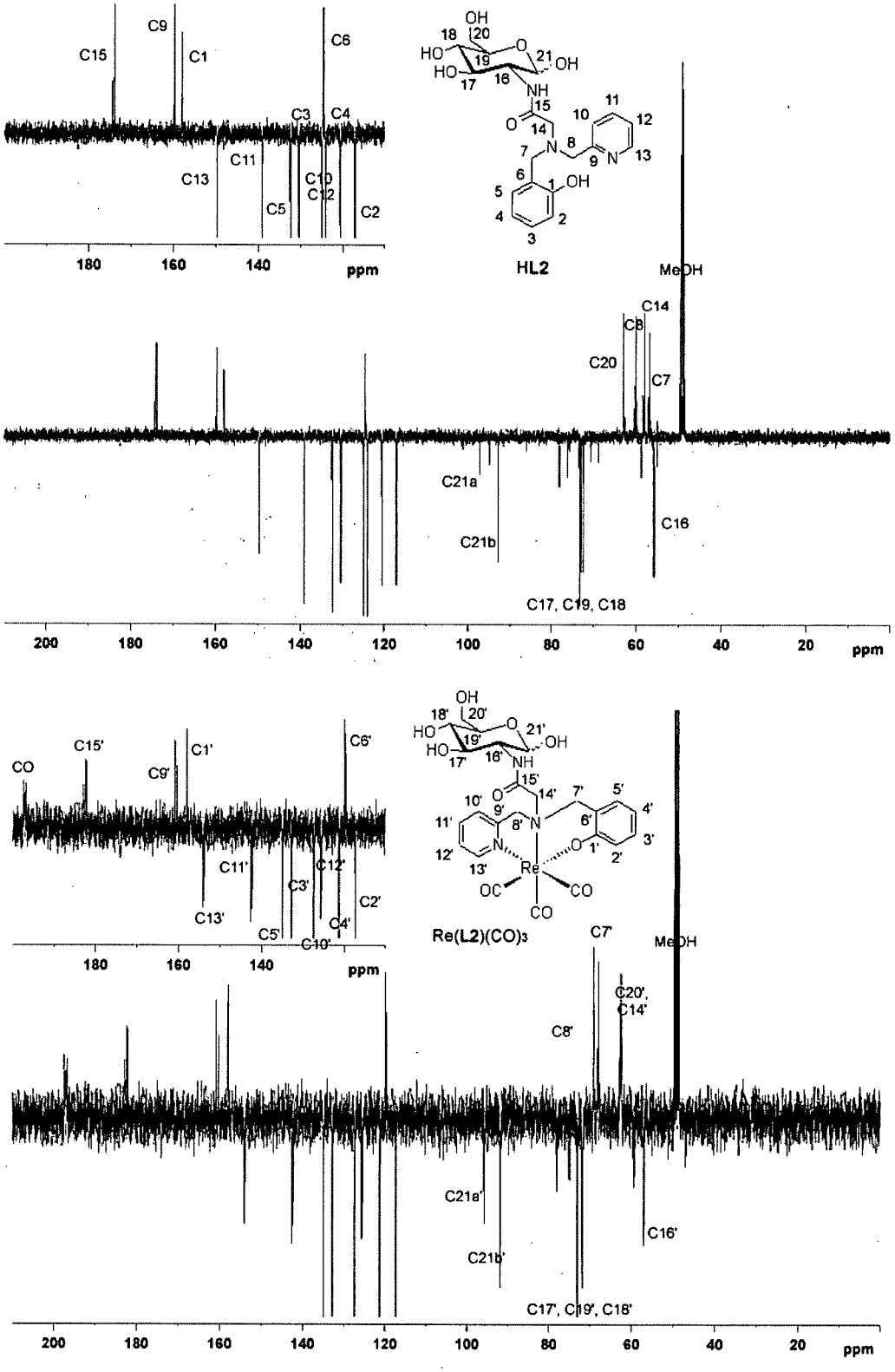

Figure 3-7. 13C APT NMR spectra (MeOH-d_4, 100 MHz, 25°C) of H**L2** and Re(**L2**)$(CO)_3$ (bottom)

C6 shift upfield (158.0 from 159.8 ppm and 119.8 from 124.6 ppm, respectively) upon binding, while the other nine carbon resonances shift downfield upon binding: C15 (174.5 to 182.8 ppm), C1 (158.0 to 160.7 ppm), C13 (149.7 to 154.0 ppm), C11 (139.0 to 142.5 ppm), C5 (132.6 to 134.9 ppm), C3 (130.3 to 132.7 ppm), C10 (124.9 to 127.4 ppm), C12 (124.1 to 125.7 ppm), C4 (120.6 to 121.2 ppm), and C2 (117.1 to 117.3 ppm). Diagnostic shifts occur for the methylene carbon resonances as well: C8 (60.5 to 69.2 ppm), C7 (56.7 to 68.2 ppm), C14 (58.1 to 62.6 ppm), whereas for C20, the resonance remains constant at 63.0 ppm (indicating the pendant nature of the glucosamine moiety, while providing evidence of binding of the tridentate unit). The other glucosamine resonances C21, C17, C19, C18, and C16 shift little, if at all, upon binding: 92.7 to 91.9 ppm, 73.2 to 73.1 ppm, to 73.0 to 72.0 ppm, 72.3 to 71.9 ppm, and 56.0 to 57.0 ppm, respectively. This confirms the pendant nature of the glucosamine and that the Re centre is indeed bound by the tridentate ligand H**L2**.

Further evidence for complex formation is provided by IR spectroscopy and mass spectrometry of dilute MeOH solutions, which corroborate the deduced solution structures. For Re(**L1**)$(CO)_3$, three bands attributable to the $[Re(CO)_3]^+$ core were present at 2203, 1909, and 1887 cm^{-1}, indicative of a low symmetry environment. For Re(**L2**)$(CO)_3$, two carbonyl bands are present at 2032 and 1905 cm^{-1}. The broader lower band at 1905 cm^{-1} is probably an overlap of two bands. Re exists as a mixture of isotopes and thus gives rise to diagnostic isotope peak patterns in the mass spectra. ES+ of Re(**L1**)$(CO)_3$ and Re(**L2**)$(CO)_3$ gave $[MH]^+$ peaks, and in addition, $[M+Na]^+$ and $[M+MeOH+Na]^+$ peaks were seen for Re(**L1**)$(CO)_3$. Such high intensity peaks provide more evidence for complex formation in solution.

3.6 Synthesis and characterization of ^{99m}Tc complexes

^{99m}Tc(**L1**)$(CO)_3$ and ^{99m}Tc(**L2**)$(CO)_3$ were prepared using the Isolink™ kit available from Mallinckrodt, Inc according to Section 2.4, page 39. As discussed earlier (Scheme 1-1, page 11), an Isolink™ kit, containing a mixture of sodium salts (tartrate, tetraborate, carbonate, and boranocarbonate) is used to prepare the precursor $[^{99m}Tc(CO)_3(H_2O)]^+$ from a saline solution of $Na[^{99m}TcO_4]$. The radiolabelling reaction scheme is shown in Scheme 3-5.

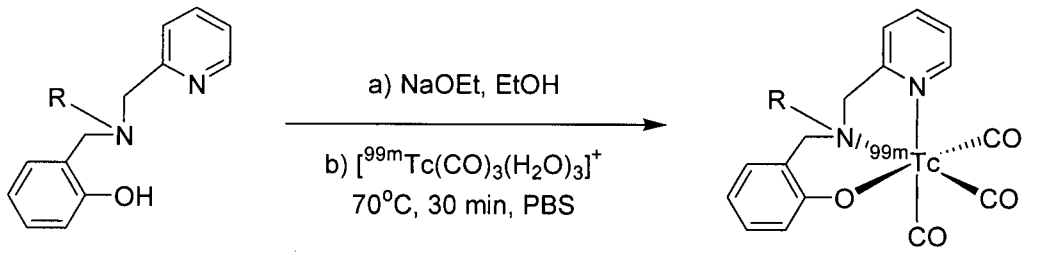

HL**1**, R = H

HL**2**, R =

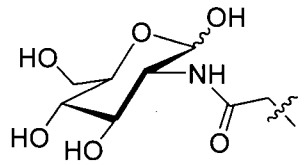

^{99m}Tc(**L1**)$(CO)_3$, R = H

^{99m}Tc(**L2**)$(CO)_3$, R =

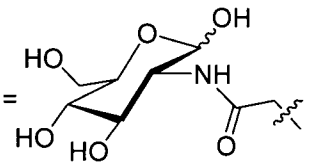

Scheme 3-5. Preparation of ^{99m}Tc complexes

To investigate the potential utility of ^{99m}Tc(**L1**)$(CO)_3$ and ^{99m}Tc(**L2**)$(CO)_3$ as imaging agents, challenge experiments are performed with aqueous amino acid solutions of cysteine and histidine in PBS (phosphate buffered saline, 0.1M, pH = 7.2) solutions. Challenge experiments are used to obtain stability information about these metal complexes. Since such complexes may someday be used as imaging agents, it is important that the metal complexes are stable

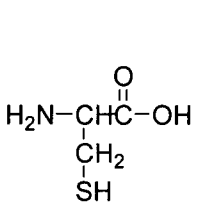

cysteine

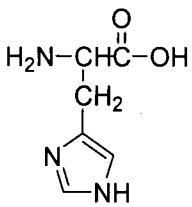

histidine

and inert to substitution by other ligand systems that are present in living systems. Since amino acids are ubiquitous in living systems, challenge experiments are performed with these potentially competing amino acids (*i.e.* cysteine and histidine). These challenge experiments resulted in ^{99m}Tc(**L1**)(CO)$_3$ and ^{99m}Tc(**L2**)(CO)$_3$ displaying excellent stability towards 100-fold excess cysteine and histidine in aqueous PBS.

Corresponding HPLC traces for radiochemical yield and cysteine/histidine challenge experiments for ^{99m}Tc(**L1**)(CO)$_3$ are shown in Figure 3-8 and those for ^{99m}Tc(**L2**)(CO)$_3$ are shown in Figure 3-9. The average radiochemical yields (as determined by the formation of only one set of peaks) for the synthesis of ^{99m}Tc(**L1**)(CO)$_3$ and ^{99m}Tc(**L2**)(CO)$_3$ were 99±1% (n = 3); representative traces are shown in Figure 3-8 a), b) and Figure 3-9 a), b) (UV and radiation traces, respectively); these traces are due to the presence and formation of Re(**L1**)(CO)$_3$/^{99m}Tc(**L1**)(CO)$_3$ and Re(**L2**)(CO)$_3$/^{99m}Tc(**L2**)(CO)$_3$, respectively. ^{99m}Tc(**L1**)(CO)$_3$ and ^{99m}Tc(**L2**)(CO)$_3$ were stable at 24h in excess cysteine or histidine solutions, indicating strong tridentate binding. The cysteine traces are represented in Figure 3-8 c), d) (for Re(**L1**)(CO)$_3$/^{99m}Tc(**L1**)(CO)$_3$) and Figure 3-9 c), d) (Re(**L2**)(CO)$_3$/^{99m}Tc(**L2**)(CO)$_3$). The histidine traces are represented in Figure 3-8 e), f) (for Re(**L1**)(CO)$_3$/^{99m}Tc(**L1**)(CO)$_3$) and Figure 3-9 e), f) (Re(**L2**)(CO)$_3$/^{99m}Tc(**L2**)(CO)$_3$). In all cases, the retention time (t_R) of the associated Re and ^{99m}Tc complexes were similar within experimental error. The instrumentation for the HPLC analysis has the radiation detector (NaI) placed after the UV-detector. Hence, the radiation traces show longer retention times than do the analogous UV traces. This is also the reason why co-injection is used; the UV-detector senses the non-radioactive Re-complexes whereas the radiation

detector senses the radioactive ^{99m}Tc-complexes. Both HPLC traces can be compared to see that the UV-trace and the radiation trace are similar. For Re(**L1**)$(CO)_3$/^{99m}Tc(**L1**)$(CO)_3$, the presence of one product is confirmed from the HPLC traces (Figure 3-8) because of the presence of single peak. In addition to the NMR spectra, the traces for Re(**L2**)$(CO)_3$ and ^{99m}Tc(**L2**)$(CO)_3$ (Figure 3-9) show two peaks, which support the evidence provided by the NMR spectra for the presence of two anomers in solution. In all cases, no other peaks were detected, hence confirming the similarity between the Re and ^{99m}Tc complexes.

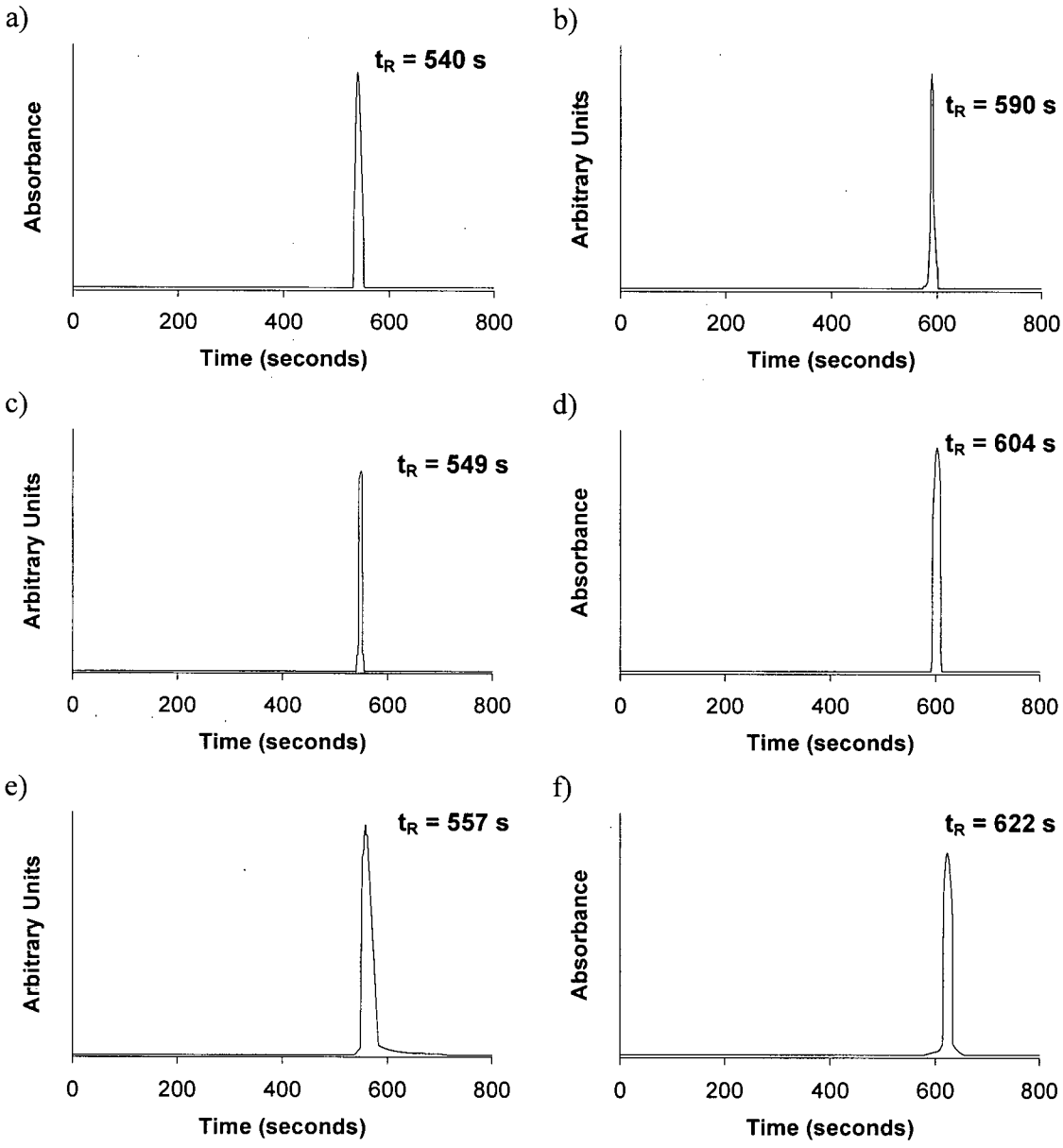

Figure 3-8. All traces are a result of co-injection of Re(**L1**)$(CO)_3$ with ^{99m}Tc(**L1**)$(CO)_3$ in EtOH/H_2O: a) UV trace; b) radiation trace; c) UV trace in cysteine solution at 24h at 25°C; d) radiation trace in cysteine solution at 24h at 25°C; e) UV trace in histidine solution at 24h at 25°C; f) radiation trace in histidine solution at 24h at 25°C.

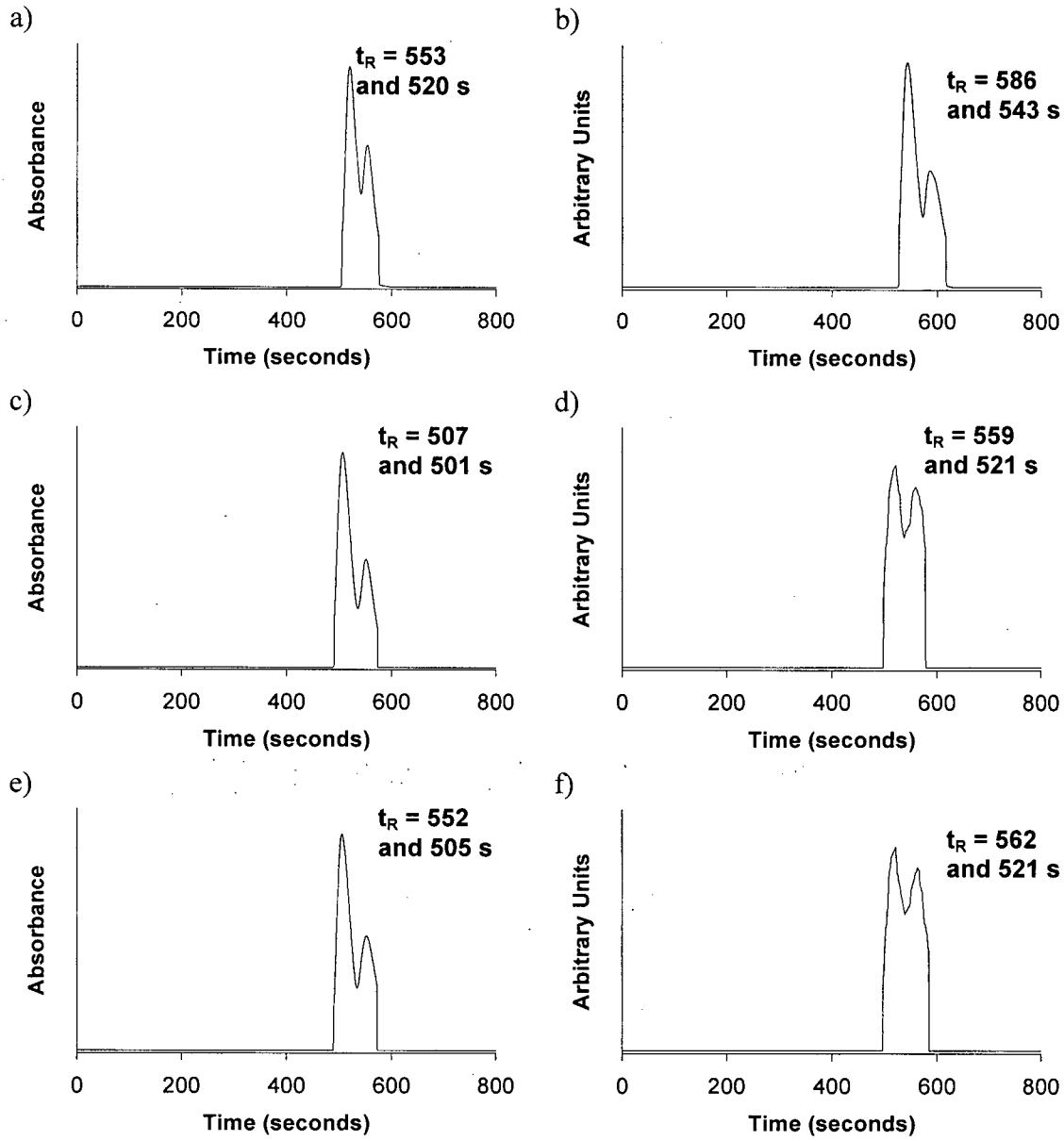

Figure 3-9. All traces are a result of co-injection of Re(**L2**)$(CO)_3$ with ^{99m}Tc(**L2**)$(CO)_3$ in EtOH/H_2O: a) UV trace; b) radiation trace; c) UV trace in cysteine solution at 24h at 25°C; d) radiation trace in cysteine solution at 24h at 25°C; e) UV trace in histidine solution at 24h at 25°C; f) radiation trace in histidine solution at 24h at 25°C.

CHAPTER 4: CONCLUSIONS AND FUTURE WORK

This thesis project has described the synthesis, characterization, and solution state behaviour of two Re-complexes, Re(**L1**)$(CO)_3$ and Re(**L2**)$(CO)_3$. The corresponding ligands, H**L1** and H**L2** respectively, were radiolabelled with the $[^{99m}Tc(CO)_3(H_2O)_3]^+$ cation via an Isolink® kit in high yields and showed excellent radiochemical yield as well as very good stability out to 24h in aqueous cysteine and histidine solutions. NMR spectroscopy provided evidence to the pendant nature of the carbohydrate in Re(**L2**)$(CO)_3$ and the existence of two anomers in solution, while mass spectrometry corroborated the proposed tridentate structures and the diagnostic fragmentation pattern of the Re complexes. IR spectroscopy provided evidence of the tricarbonyl functionality for Re(**L1**)$(CO)_3$ and Re(**L2**)$(CO)_3$.

Such a ligand design exhibits functional utility. The carbohydrate could be replaced with glucosamine diastereomers (*e.g.* galactosamine and mannosamine), the amide bond could be replaced with an amine bond, the glycine spacer could be extended with various CH_2 lengths, and the tridentate arms could be replaced with an imidazole and/or a carboxylate functionality. Compound **31**, shown here, with its *t*-butoxide protecting group, could be used as a precursor for a monoprotic carboxylate arm. Other designs could employ a suitable protected histidine moiety to link up to such a carbohydrate scaffold. Animal studies could also be used to determine the utility of such carbohydrate compounds as potential imaging agents *in vivo*.

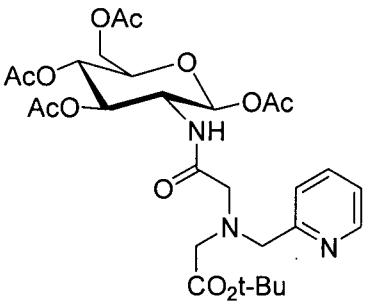

31

References

1. Orvig, C.; Abrams, M. J. *Chem. Rev.* **1999**, *99*, 2201-2203.

2. Caravan, P.; Ellison, J. J.; McMurry, T. J.; Lauffer, R. B. *Chem. Rev.* **1999**, *99*, 2293-2352.

3. Lehninger, A. L.; Nelson, D. L.; Cox, M. M. **1993**.

4. Brown, G. K. *Journal of Inherited Metabolic Disease* **2000**, *23*, 237-246.

5. Wood, I. S.; Trayhurn, P. *Br. J. Nutr.* **2003**, *89*, 3-9.

6. Uldry, M.; Ibberson, M.; Hosokawa, M.; Thorens, B. *FEBS Lett.* **2002**, *524*, 199-203.

7. Schibli, R.; La Bella, R.; Alberto, R.; Garcia-Garayoa, E.; Ortner, K.; Abram, U.; Schubiger, P. A. *Bioconjugate Chem.* **2000**, *11*, 345-351.

8. Liu, S. *Chem. Soc. Rev.* **2004**, *33*, 445-461.

9. Volkert, W. A.; Hoffman, T. J. *Chem. Rev.* **1999**, *99*, 2269-2292.

10. Thompson, K. H.; Orvig, C. *Science* **2003**, *300*, 936-939.

11. Bailey, D. L.; Adamson, K. L. *Curr. Pharm. Des.* **2003**, *9*, 903-916.

12. Bayly, S. R.; Fisher, C. L.; Storr, T.; Adam, M. J.; Orvig, C. *Bioconjugate Chem.* **2004**, *15*, 923-926.

13. Storr, T.; Fisher, C. L.; Mikata, Y.; Yano, S.; Adam, M. J.; Orvig, C. *Dalton Trans.* **2005**, 654-655.

14. Storr, T.; Obata, M.; Fisher, C. L.; Bayly, S. R.; Green, D. E.; Brudzinska, I.; Mikata, Y.; Patrick, B. O.; Adam, M. J.; Yano, S.; Orvig, C. *Chem. Eur. J.* **2004**, *11*, 195-203.

15. Storr, T.; Sugai, Y.; Barta, C. A.; Mikata, Y.; Adam, M. J.; Yano, S.; Orvig, C. *Inorg. Chem.* **2005**, *44*, 2698-2705.

16. Anderson, C. J.; Welch, M. J. *Chem. Rev.* **1999**, *99*, 2219-2234.

17. Fowler, J. S.; Wolf, A. P. *Acc. Chem. Res.* **1997**, *30*, 181-188.

18. Zhang, M.; Zhang, Z. H.; Blessington, D.; Li, H.; Busch, T. M.; Madrak, V.; Miles, J.; Chance, B.; Glickson, J. D.; Zheng, G. *Bioconjugate Chem.* **2003**, *14*, 709-714.

19. Adam, M. J. *J. Labelled Compd. Radiopharm.* **2002**, *45*, 167-180.

20. Dilworth, J. R.; Parrott, S. J. *Chem. Soc. Rev.* **1998**, *27*, 43-55.

21. Jurisson, S. S.; Lydon, J. D. *Chem. Rev.* **1999**, *99*, 2205-2218.

22. Schwochau, K. *Angew. Chem. Int. Ed. Engl.* **1994**, *33*, 2258-2267.

23. Alberto, R.; Schibli, R.; Egli, A.; Schubiger, A. P.; Abram, U.; Kaden, T. A. *J. Am. Chem. Soc.* **1998**, *120*, 7987-7988.

24. Blauenstein, P. *New J. Chem.* **1990**, *14*, 405-407.

25. Alberto, R.; Schibli, R.; Waibel, R.; Abram, U.; Schubiger, A. P. *Coord. Chem. Rev.* **1999**, *192*, 901-919.

26. Banerjee, S. R.; Maresca, K. P.; Francesconi, L.; Valliant, J.; Babich, J. W.; Zubieta, J. *Nucl. Med. Biol.* **2005**, *32*, 1-20.

27. Jaouen, G.; Top, S.; Vessieres, A.; Alberto, R. *J. Organomet. Chem.* **2000**, *600*, 23-36.

28. Schibli, R.; Schubiger, P. A. *European Journal of Nuclear Medicine and Molecular Imaging* **2002**, *29*, 1529-1542.

29. Alberto, R.; Ortner, K.; Wheatley, N.; Schibli, R.; Schubiger, A. P. *J. Am. Chem. Soc.* **2001**, *123*, 3135-3136.

30. Alberto, R. *Eur. J. Nucl. Med. Mol. Imaging* **2003**, *30*, 1299-1302.

31. van Staveren, D. R.; Mundwiler, S.; Hoffmanns, U.; Pak, J. K.; Spingler, B.; Metzler-Nolte, N.; Alberto, R. *Org. Biomol. Chem.* **2004**, *2*, 2593-2603.

32. Mundwiler, S.; Kundig, M.; Ortner, K.; Alberto, R. *Dalton Trans.* **2004**, 1320-1328.

33. Schibli, R.; Katti, K. V.; Higginbotham, C.; Volkert, W. A.; Alberto, R. *Nucl. Med. Biol.* **1999**, *26*, 711-716.

34. Pietzsch, H. J.; Gupta, A.; Reisgys, M.; Drews, A.; Seifert, S.; Syhre, R.; Spies, H.; Alberto, R.; Abram, U.; Schubiger, P. A.; Johannsen, B. *Bioconjugate Chem.* **2000**, *11*, 414-424.

35. Hafliger, P.; Mundwiler, S.; Ortner, K.; Spingler, B.; Alberto, R.; Andocs, G.; Balogh, L.; Bodo, K. *Synth. React. Inorg., Met.-Org., Nano-Met. Chem.* **2005**, *35*, 27-34.

36. Alberto, R.; Pak, J. K.; van Staveren, D.; Mundwiler, S.; Benny, P. *Biopolymers* **2004**, *76*, 324-333.

37. Lazarova, N.; Babich, J.; Valliant, J.; Schaffer, P.; James, S.; Zubieta, J. *Inorg. Chem.* **2005**, *44*, 6763-6770.

38. Liu, G. Z.; Dou, S. P.; He, J.; Vanderheyden, J. L.; Rusckowski, M.; Hnatowich, D. J. *Bioconjugate Chem.* **2004**, *15*, 1441-1446.

39. Santos, I. G.; Abram, U.; Alberto, R.; Lopez, E. V.; Sanchez, A. *Inorg. Chem.* **2004**, *43*, 1834-1836.

40. Banerjee, S. R.; Schaffer, P.; Babich, J. W.; Valliant, J. F.; Zubieta, J. *Dalton Trans.* **2005**, 3886-3897.

41. Banerjee, S. R.; Babich, J. W.; Zubieta, J. *Chem. Commun.* **2005**, 1784-1786.

42. van Staveren, D. R.; Benny, P. D.; Waibel, R.; Kurz, P.; Pak, J. K.; Alberto, R. *Helv. Chim. Acta.* **2005**, *88*, 447-460.

43. Sogbein, O. O.; Green, A. E. C.; Valliant, J. F. *Inorg. Chem.* **2005**, *44*, 9585-9591.

44. Stichelberger, A.; Waibel, R.; Dumas, C.; Schubiger, P. A.; Schibli, R. *Nucl. Med. Biol.* **2003**, *30*, 465-470.

45. Stephenson, K. A.; Banerjee, S. R.; Sogbein, O. O.; Levadala, M. K.; McFarlane, N.; Boreham, D. R.; Maresca, K. P.; Babich, J. W.; Zubieta, J.; Valliant, J. F. *Bioconjugate Chem.* **2005**, *16*, 1189-1195.

46. Stephenson, K. A.; Zubieta, J.; Banerjee, S. R.; Levadala, M. K.; Taggart, L.; Ryan, L.; McFarlane, N.; Boreham, D. R.; Maresca, K. P.; Babich, J. W.; Valliant, J. F. *Bioconjugate Chem.* **2004**, *15*, 128-136.

47. Waibel, R.; Alberto, R.; Willuda, J.; Finnern, R.; Schibli, R.; Stichelberger, A.; Egli, A.; Abram, U.; Mach, J. P.; Pluckthun, A.; Schubiger, P. A. *Nat. Biotechnol.* **1999**, *17*, 897-901.

48. Pak, J. K.; Benny, P.; Spingler, B.; Ortner, K.; Alberto, R. *Chem. Eur. J.* **2003**, *9*, 2053-2061.

49. Egli, A.; Alberto, R.; Tannahill, L.; Schibli, R.; Abram, U.; Schaffland, A.; Waibel, R.; Tourwe, D.; Jeannin, L.; Iterbeke, K.; Schubiger, P. A. *J. Nucl. Med.* **1999**, *40*, 1913-1917.

50. van Staveren, D. R.; Waibel, R.; Mundwiler, S.; Schubiger, P. A.; Alberto, R. *J. Organomet. Chem.* **2004**, *689*, 4803-4810.

51. Banerjee, S. R.; Babich, J. W.; Zubieta, J. *Inorg. Chem. Commun.* **2004**, *7*, 481-484.

52. Levadala, M. K.; Banerjee, S. R.; Maresca, K. P.; Babich, J. W.; Zubieta, J. *Synthesis* **2004**, 1759-1766.

53. Stephenson, K. A.; Banerjee, S. R.; Besanger, T.; Sogbein, O. O.; Levadala, M. K.; McFarlane, N.; Lemon, J. A.; Boreham, D. R.; Maresca, K. P.; Brennan, J. D.; Babich, J. W.; Zubieta, J.; Valliant, J. F. *J. Am. Chem. Soc.* **2004**, *126*, 8598-8599.

54. Banerjee, S. R.; Babich, J. W.; Zubieta, J. *Inorg. Chim. Acta* **2006**, *359*, 1603-1612.

55. Petrig, J.; Schibli, R.; Dumas, C.; Alberto, R.; Schubiger, P. A. *Chem. Eur. J.* **2001**, *7*, 1868-1873.

56. Yang, D. J.; Kim, C. G.; Schechter, N. R.; Azhdarinia, A.; Yu, D. F.; Oh, C. S.; Bryant, J. L.; Won, J. J.; Kim, E. E.; Podoloff, D. A. *Radiology* **2003**, *226*, 465-473.

57. Lazarova, N.; James, S.; Babich, J.; Zubieta, J. *Inorg. Chem. Commun.* **2004**, *7*, 1023-1026.

58. Schibli, R.; Schwarzbach, R.; Alberto, R.; Ortner, K.; Schmalle, H.; Dumas, C.; Egli, A.; Schubiger, P. A. *Bioconjugate Chem.* **2002**, *13*, 750-756.

59. Banerjee, S. R.; Wei, L. H.; Levadala, M. K.; Lazarova, N.; Golub, V. O.; O'Connor, C. J.; Stephenson, K. A.; Valliant, J. F.; Babich, J. W.; Zubieta, J. *Inorg. Chem.* **2002**, *41*, 5795-5802.

60. Abdel-Magid, A. F.; Carson, K. G.; Harris, B. D.; Maryanoff, C. A.; Shah, R. D. *J. Org. Chem.* **1996**, *61*, 3849-3862.

61. Policar, C.; Durot, S.; Lambert, F.; Cesario, M.; Ramiandrasoa, F.; Morgenstern-Badarau, I. *Eur. J. Inorg. Chem.* **2001**, 1807-1818.

62. Policar, C.; Lambert, F.; Cesario, M.; Morgenstern-Badarau, I. *Eur. J. Inorg. Chem.* **1999**, 2201-2207.

63. Dumas, C.; Petrig, J.; Frei, L.; Spingler, B.; Schibli, R. *Bioconjugate Chem.* **2005**, *16*, 421-428.

64. Schibli, R.; Dumas, C.; Petrig, J.; Spadola, L.; Scapozza, L.; Garcia-Garayoa, E.; Schubiger, P. A. *Bioconjugate Chem.* **2005**, *16*, 105-112.

65. Adam, M. J.; Hall, L. D. *Can. J. Chem.* **1982**, *60*, 2229-2237.

66. Duatti, A.; Marchi, A.; Magon, L.; Deutsch, E.; Bertolasi, V.; Gilli, G. *Inorg. Chem.* **1987**, *26*, 2182-2186.

67. Breitenmoser, R. A.; Heimgartner, H. *Helv. Chim. Acta.* **2001**, *84*, 786-796.

68. Silva, D. J.; Wang, H. M.; Allanson, N. M.; Jain, R. K.; Sofia, M. J. *J. Org. Chem.* **1999**, *64*, 5926-5929.

69. Johansson, A.; Abrahamsson, M.; Magnuson, A.; Huang, P.; Martensson, J.; Styring, S.; Hammarstrom, L.; Sun, L. C.; Akermark, B. *Inorg. Chem.* **2003**, *42*, 7502-7511.

70. Kolodziuk, R.; Penciu, A.; Tollabi, M.; Framery, E.; Goux-Henry, C.; Iourtchenko, A.; Sinou, D. *J. Organomet. Chem.* **2003**, *687*, 384-391.

71. Parisot, S.; Kolodziuk, R.; Goux-Henry, C.; Iourtchenko, A.; Sinou, D. *Tetrahedron Lett.* **2002**, *43*, 7397-7400.

72. Tollabi, M.; Framery, E.; Goux-Henry, C.; Sinou, D. *Tetrahedron-Asymmetr* **2003**, *14*, 3329-3333.

73. Banerjee, S. R.; Levadala, M. K.; Lazarova, N.; Wei, L. H.; Valliant, J. F.; Stephenson, K. A.; Babich, J. W.; Maresca, K. P.; Zubieta, J. *Inorg. Chem.* **2002**, *41*, 6417-6425.

74. Gathergood, N.; Scammells, P. J. *Org. Lett.* **2003**, *5*, 921-923.

75. Shu, L. H.; Shen, Y. M.; Burke, C.; Goeddel, D.; Shi, Y. *J. Org. Chem.* **2003**, *68*, 4963-4965.

76. Bednarski, M.; Danishefsky, S. *J. Am. Chem. Soc.* **1986**, *108*, 7060-7067.